Review

Effective Quantum Field Theory Methods for Calculating Feynman Integrals

Anatoly V. Kotikov

Bogoliubov Laboratory of Theoretical Physics, Joint Institute for Nuclear Research, 141980 Dubna, Russia; kotikov@theor.jinr.ru

Abstract: A review of modern methods for effective calculations of Feynman integrals containing both massless propagators and propagators with masses is given. The effectiveness of these methods in various fields of their application is demonstrated by the examples under consideration.

1. Introduction

Currently, perturbation theory (PT) provides basic information about both the processes studied in experiments and the properties of the physical models themselves. The matrix elements in the cross-sections of the processes depend on the masses of the interacting particles, and therefore, strictly speaking, require the calculation of Feynman integrals (FIs) containing massive propagators. However, depending on the kinematics of the processes under study, the values of some masses can be set to zero, and then the FI calculation is greatly simplified.

Studying the properties of the physical models themselves, such as critical indices, anomalous dimensions for particles, and operators, requires the calculations of massless FIs, whose results contain fairly simple structures. These results can be obtained in PT high orders.

FI calculations are preferably, if possible, analytical methods, since numerical methods rarely have sufficiently high accuracy. In addition, numerical methods for calculating diagrams are often inapplicable due to the singularities they contain and (which is especially important for gauge theories) due to mutual reductions between the contributions of different integrals and even between different parts of the same integral.

Moreover, accurate results are often needed. For example, when calculating renormalizations in theories with high internal symmetry, it is important to know [1] the positions of critical points in which the found β functions have zero values in the appropriate PT order.

I would like to draw attention to the fact that the main objects of calculations are scalar diagrams. Therefore, within the framework of dimensional regularization [2–5], where diagrams are calculated for an arbitrary dimension of space, the FIs found for any model (or process) can be easily used in the study of other models (and processes). As a result, the complexity of the analytical FI calculations is compensated by the possibility of their application in various quantum field models.

We also note that sometimes the result of FI calculations may be of independent interest. So, for example, when using non-trivial identities such as the "uniqueness" relation [6,7], the results appear (see [8–13]) for some integrals and/or series that are not available in the reference literature. For example, the calculation of the same FI performed in [8–12] and [14] using various calculation methods, led to a previously unknown relation between $_3F_2$-hypergeometric functions with arguments 1 and -1. This ratio was neatly proven only very recently [15].

Now there are many powerful methods for calculating the Feynman diagrams of a certain type (in the massless and massive cases (see, in particular, recent reviews in [16,17],

respectively), which are often inferior in breadth of use to standard methods such as α-representation and the Feynman parameter method (see, for example, [1,18]); however, this lead to significant progress in studying specific processes (or quantities).

In this review, we will present methods based on integration by parts (IBP) [7,19], on functional relations (FRs) [20–22], and on differential equations (DEs) [23–29], which are conveniently applicable when calculating both massless diagrams and diagrams with massive propagators. In the massless case, we will consider, in particular, diagrams giving contributions to the coefficient functions and anomalous dimensions of Wilson operators in the framework of deep inelastic scattering (DIS) of leptons on hadrons (see Sections 1–4).

Moreover, we will also consider the basic diagrams that contribute to the β function of the φ^4 model, two of which will be five-loop. When calculating [30] a five-loop correction to the β function of the φ^4 model, the results of the four FIs were only numerically calculated. The analytical results for these diagrams were obtained by Kazakov (see [8–12]); however, they were published without presenting any intermediate results. Moreover, all calculations were performed by Kazakov in x-space, which makes them difficult to understand. In Section 5, we provide an accurate calculation of two of the four diagrams.

Calculations of the massive diagrams are given in Sections 6–8. The rules of their effective calculation are presented, and examples of calculating two- and three-point diagrams are given. Recurrent relations for the coefficients of the reverse expansion of the mass are presented. A brief overview of modern computer technologies is also given.

Section 7 provides calculations of one of the main integrals that contribute to the ratio between the $\overline{MS}$-mass and the pole mass of the Higgs boson in the standard model in the heavy Higgs limit.

To obtain results for the most complex parts of massless and massive diagrams, recurrence relations are used for their decomposition coefficients (as can also be seen in Section 8); (at present, recursive relations (see [31–35]) for diagrams with different space values are also popular, but their consideration is beyond the scope of this article.).

Solving these recursive dependencies, we obtain accurate results for these most difficult parts.

We also discuss the popular property of maximum transcendentality. The most popular introduction to this property was in [36] for the kernel of the Balitsky–Fadin–Kuraev–Lipatov (BFKL) Equation [37–44] in the case of the $\mathcal{N} = 4$ supersymmetric Yang model-Mills (SIM) model [45,46]. This property is also applicable to the matrix of anomalous dimensions of the Wilson operators [47–50] and for the Wilson coefficients [51] of the "deep inelastic scattering" in this model after their corresponding diagonalization. This property allows one to obtain results for both anomalous dimensions and coefficient functions without any direct calculations, but simply using the corresponding values obtained in QCD [52–54].

In Section 8, we also show the presence of the property of maximum transcendentality (or maximum complexity) in the results of two-loop two- and three-point FIs (see also [55–59] and a review in [60]).

Indeed, this property manifests itself in the results of computing a large FI class, mainly for the so-called master integrals (MIs) [61]. For most of the MIs, the results can be reconstructed without direct calculations, but using the knowledge of several coefficients in their inverse mass expansion [62] (as can also be seen in [63] and the references and discussions therein). Note that similar properties are also demonstrated in the calculations of amplitudes, form factors, and correlation functions (see [64–76] and references to them), as performed in $\mathcal{N} = 4$ SYM.

2. Basic Formulas

Now, we consider the rules for calculating massless FIs. All calculations are performed in the momentum Euclidean space.

Following [14,77], we present the traceless product (TP) $q^{\mu_1\mu_2\mu_3\cdots\mu_n}$ with $g^{\mu_i\mu_j}q^{\mu_1\mu_2\mu_3\cdots\mu_n} = 0$ $(i,j = 1,2,3,...n)$ of the momenta associated with the standard product $q^{\mu_1}q^{\mu_2}q^{\mu_3}...q^{\mu_n}$ as follows

$$q^{\mu_1\mu_2\mu_3\cdots\mu_n} = \hat{S} \sum_{p\geq 0} \frac{(-1)^p n!\Gamma(n-p+\lambda)}{2^{2p}(n-2p)!p!\Gamma(n+\lambda)} g^{\mu_1\mu_2}g^{\mu_3\mu_4}...g^{\mu_{2p-1}\mu_{2p}} q^{2p} q^{\mu_{2p+1}}q^{\mu_{2p+2}}q^{\mu_{2p+3}}...q^{\mu_n} ,$$

$$q^{\mu_1}q^{\mu_2}q^{\mu_3}...q^{\mu_n} = \hat{S} \sum_{p\geq 0} \frac{n!\Gamma(n-2p+1+\lambda)}{2^{2p}(n-2p)!p!\Gamma(n-p+1+\lambda)} g^{\mu_1\mu_2}g^{\mu_3\mu_4}...g^{\mu_{2p-1}\mu_{2p}} q^{2p} q^{\mu_{2p+1}\mu_{2p+2}\mu_{2p+3}\cdots\mu_n} , \tag{1}$$

where the symbol $\hat{S}$ shows the symmetrization over the indices μ_i $(i = 1,2,3,...n)$.

We also present useful properties of the TP $q^{\mu_1\mu_2\mu_3\cdots\mu_n}$:

$$(q_1 q_2)^{(n)} \equiv q_1^{\mu_1\mu_2\mu_3\cdots\mu_n} q_2^{\mu_1\mu_2\mu_3\cdots\mu_n} = q_1^{\mu_1}q_1^{\mu_2}q_1^{\mu_3}...q_1^{\mu_n} q_2^{\mu_1\mu_2\mu_3\cdots\mu_n} = q_1^{\mu_1\mu_2\mu_3\cdots\mu_n} q_2^{\mu_1}q_2^{\mu_2}q_2^{\mu_3}...q_2^{\mu_n} , \tag{2}$$

which directly follow from its definition given above: $g^{\mu_i\mu_j}q^{\mu_1\mu_2\mu_3\cdots\mu_i\cdots\mu_j\cdots\mu_n} = 0$ $(i,j = 1,2,3,...,n)$.

Graphically, the propagators are presented in the form

$$\frac{1}{(q^2)^\alpha} \equiv \frac{1}{q^{2\alpha}} = \underset{\overrightarrow{q} \quad \alpha}{\bullet\!\!-\!\!-\!\!-\!\!-\!\!\bullet} \quad , \quad \frac{q^\mu}{q^{2\alpha}} = \underset{\overrightarrow{q} \quad \alpha}{\overset{\mu}{\bullet\!\!-\!\!\to\!\!-\!\!\bullet}} \quad ,$$

$$\frac{q^{\mu_1}q^{\mu_2}q^{\mu_3}...q^{\mu_n}}{q^{2\alpha}} = \underset{\overrightarrow{q} \quad \alpha}{\overset{n}{\bullet\!\!-\!\!\to\!\!-\!\!\bullet}} \quad , \quad \frac{q^{\mu_1\mu_2\mu_3\cdots\mu_n}}{q^{2\alpha}} \underset{\overrightarrow{q} \quad \alpha}{\overset{(n)}{\bullet\!\!-\!\!\to\!\!-\!\!\bullet}} \quad , \tag{3}$$

Using the TP $q^{\mu_1\cdots\mu_n}$ allows one to neglect contributions proportional to $g^{\mu_i\mu_j}$ that occur during integration: these can be easily restored based on the general TP structure.

Here as well as subsequently, integrations are performed in $d = 4 - 2\varepsilon$-space, according to the arguments $k, k_1, k_2, ...$ So, the labels $k, k_1, k_2...$ denote internal momenta. The characters $q, q_1, q_2...$ and $p, p_1, p_2...$ denote external momenta with conditions $p^2 = 0, p_1^2 = 0, p_2^2 = 0...$, respectively.

The following formulas are valid [20–22]. TP also was used to calculate complicated integrals in another way. One propagator of a complicated integral can be decomposed into an infinite sum of the products of two other propagators having TPs in their numerators (see Refs. [14,77–85] and the review [86]).

A. A chain can be represented as:

$$\frac{q^{\mu_1}q^{\mu_2}q^{\mu_3}...q^{\mu_n}}{q^{2\alpha_1}} \frac{q^{\nu_1}q^{\nu_2}q^{\nu_3}...q^{\nu_m}}{q^{2\alpha_2}} = \frac{q^{\mu_1}q^{\mu_2}q^{\mu_3}...q^{\mu_n}q^{\nu_1}q^{\nu_2}q^{\nu_3}...q^{\nu_m}}{q^{2(\alpha_1+\alpha_2)}} ,$$

or graphically

$$\underset{\overrightarrow{q} \quad \alpha_1}{\overset{n}{\bullet\!\!-\!\!\to\!\!-\!\!\bullet}}\underset{\alpha_2}{\overset{m}{-\!\!\to\!\!-\!\!\bullet}} = \underset{\overrightarrow{q} \quad \alpha_1+\alpha_2}{\overset{n+m}{\bullet\!\!-\!\!\to\!\!-\!\!\bullet}} , \tag{4}$$

that is, the propagator's product is equivalent to a new propagator with an index (the index is the power of the square of the propagator's momentum) equal to the sum of the indices of the original propagators. The number of momenta products in the numerator is equal to the sum of momenta products in the original propagators.

B. The simplest two-point diagram (loop) is integrated as

$$\int \frac{Dk\, k^{\mu_1} k^{\mu_2} k^{\mu_3}...k^{\mu_n}}{(q-k)^{2\alpha_1} k^{2\alpha_2}} = N_d \frac{q^{\mu_1}q^{\mu_2}q^{\mu_3}...q^{\mu_n}}{q^{2(\alpha_1+\alpha_2-d/2)}} A^{0,n}(\alpha_1,\alpha_2) + ... , \tag{5}$$

where we omit the terms of the order $g^{\mu_i\mu_j}$. Here

$$Dk = \frac{d^d k}{(2\pi)^d}, N_d = \frac{1}{(4\pi)^{d/2}} \tag{6}$$

is usual a Euclidean measure and

$$A^{n,m}(\alpha, \beta) = \frac{a_n(\alpha) a_m(\beta)}{a_{n+m}(\alpha + \beta - d/2)}, \quad a_n(\alpha) = \frac{\Gamma(\tilde{\alpha} + n)}{\Gamma(\alpha)}, \quad \tilde{\alpha} = \frac{d}{2} - \alpha. \tag{7}$$

It is convenient to present Equation (5) in the graphical form as follows

$$= N_d \; A^{0,n}(\alpha_1, \alpha_2) \quad \xrightarrow[\alpha_1 + \alpha_2 - d/2]{n} \quad + \ldots, \tag{8}$$

For the loop with the TP $k^{\mu_1 \mu_2 \mu_3 \ldots \mu_n}$, we have

$$\int \frac{Dk \, k^{\mu_1 \mu_2 \mu_3 \ldots \mu_n}}{(q-k)^{2\alpha_1} k^{2\alpha_2}} = N_d \, \frac{q^{\mu_1 \mu_2 \mu_3 \ldots \mu_n}}{q^{2(\alpha_1 + \alpha_2 - d/2)}} \, A^{0,n}(\alpha_1, \alpha_2), \tag{9}$$

or graphically

$$= N_d \, A^{0,n}(\alpha_1, \alpha_2) \quad \xrightarrow[\alpha_1 + \alpha_2 - D/2]{(n)} \quad , \tag{10}$$

As noted above, indeed, in Equation (9), we used the TP $q^{\mu_1 \ldots \mu_n}$, so in fact we only need the first term of r.h.s. of Equation (5) $\sim q^{\mu_1} \ldots q^{\mu_n}$, because the rest of the result in Equation (9) is exactly recoverable from the TP exact form. This property can be shown in another way: the results (9) and (10) can also be obtained using an additional light-like momentum u (i.e., with $u^2 = 0$) and taking into account the property $(uk)^n = u_{\mu_1} \ldots u_{\mu_n} k^{\mu_1} \ldots k^{\mu_n} = u_{\mu_1} \ldots u_{\mu_n} k^{\mu_1 \ldots \mu_n}$, because $u^2 = 0$.

So, the result (9) has the following form

$$\int \frac{Dk \, (uk)^n}{(q-k)^{2\alpha_1} k^{2\alpha_2}} = N_d \, \frac{(uq)^n}{q^{2(\alpha_1 + \alpha_2 - d/2)}} \, A^{0,n}(\alpha_1, \alpha_2),$$

or graphically

$$= N_d \, A^{0,n}(\alpha_1, \alpha_2) \, (u_{\mu_1} \ldots u_{\mu_n}) \quad \xrightarrow[\alpha_1 + \alpha_2 - D/2]{n} \quad . \tag{11}$$

Note that we use all μ_i belonging to TP, i.e., we consider the case of TP inside the scalar diagrams. In theories such as QCD, there are still other indices λ_j that arise from the propagator's numerators. In such cases, we cannot neglect the terms $g^{\lambda_i \lambda_j}$ and $g^{\mu_i \lambda_j}$, and consequently, the rules for integration become more complicated (they were considered in [20–22]).

Thus, diagrams that can be represented as combinations of loops and chains can be immediately calculated by applying the Equations (4) and (10) discussed above. However, starting from the two-loop level, diagrams appear that are not expressed as combinations of loops and chains (the simplest example is shown below in Figure 1). For such cases, there are additional rules that are shown below only graphically to increase their visibility.

C. When $\sum \alpha_i = d$, there is a so-called uniqueness relation [6–12] for the triangle with indices α_i ($i = 1, 2, 3$)

$$\stackrel{\sum \alpha_i = d}{=} N_d \sum_{m=0}^{n} C_n^m A^{n-m,m}(\alpha_2, \alpha_3) \qquad (12)$$

where

$$C_n^m = \frac{n!}{m!(n-m)!}. \qquad (13)$$

Results (12) can be precisely obtained as follows: perform the inversion $q_i \to 1/q_i$ ($i = 1, 2, 3$), $k \to 1/k$ in the integrand and in the integral measure. Inversion preserves the angles between momenta. After the inversion, one propagator disappears, because $\sum \alpha_i = d$, and the considered triangle turns into a loop. Calculating the loop using (8) and returning it to the original momenta, we obtain the rule (12). Its extension to the case of two TPs can be found in [22].

D. For any triangle with indices α_i ($i = 1, 2, 3$), there is the following relation based on the IBP procedure [7,19,87] (for non-zero n, m, and k values, Equation (14) was obtained in Refs. [20–22].)

$$(d - 2\alpha_1 - \alpha_2 - \alpha_3 + n + m + k)$$

$$= \alpha_2 \Bigg[\qquad - (q_2 - q_1)^2 \times \qquad (14)$$

$$+ m(q_2 - q_1)^{\mu_m} \times \qquad \Bigg] + \alpha_3 \Big[\alpha_2 \leftrightarrow \alpha_3, m \leftrightarrow k \Big].$$

The result (14) can been obtained by introducing the factor $(\partial/\partial k_\mu)(k - q_1)^\mu = d$ to the integrand of the triangle, shown below as [...], and using the IBP procedure as follows:

$$d \int Dk\,[...] = \int Dk \left(\frac{\partial}{\partial k_\mu}(k - q_1)^\mu \right)[...] = \int Dk \frac{\partial}{\partial k_\mu}\left((k - q_1)^\mu\,[...] \right)$$

$$- \int Dk\,(k - q_1)^\mu \frac{\partial}{\partial k_\mu}\left([...] \right) \qquad (15)$$

The first term in the r.h.s. is zero, because it can be represented as a surface integral on an infinite surface. By calculating the second term in the r.h.s., we reproduce Equation (14).

As can be seen from Equations (14) and (15), the line with the index α_1 is distinguished. The dependence on the indexes of the other line is the same. So, we will call the line with the index α_1 as the "distinguished line". It is clear that the different selection of the distinguished line in the triangles of a diagram leads to different types of IBP relations.

Using the IBP relation (14) allows someone to change FI indexes by an integer. FI indexes can also be changed using a transformation group [7,88,89] with the elements:

(a) Transition to a coordinate representation;
(b) Conformal inversion transformation $p \to p' = p/p^2$;
(c) A special series of transformations that allows someone to make one of the vertices unique, and then apply the relation (12) to it.

The extension of the transformation group for diagrams with a TP can be found in Ref. [22].
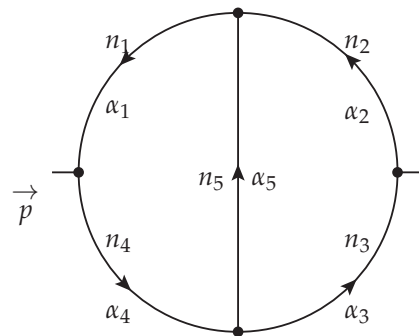
Figure 1. FI which cannot be expressed as a combination of loops and chains.

3. Basic Massless Two-Loop FIs

The general topology of the two-loop two-point FI, which cannot be expressed as a combinations of loops and chains, is shown in Figure 1.

Below, we will mainly focus on two special cases of the FI shown in Figure 1, for $\alpha_3 + n_3 = \alpha$, $n_3 = n$, $\alpha_j(j \neq 3) = 1$, $n_j(j \neq 3) = 0$ (denote by $I_1(\alpha, n)$) and for $\alpha_5 + n_5 = \alpha$, $n_5 = n$, $\alpha_j(j \neq 5) = 1$, $n_j(j \neq 5) = 0$ (denote by $I_2(\alpha, n)$)

$$I_1(\alpha, n) = \quad , \quad I_2(\alpha, n) = \qquad\qquad (16)$$

We will calculate the diagrams $I_1(\alpha, n)$ and $I_2(\alpha, n)$ using FRs similar to those obtained [13,90]. (such FRs were obtained in [13,90] by applying IBP relations to various highlighted lines.) This greatly reduces the amount of calculations.

Repeating the analysis performed in [13], we obtain the following FRs:

$$I_1(\alpha, n) = \frac{1}{q^2} I_1(\alpha - 1, n) - \frac{1}{2\varepsilon} \left(2I_{1,1}(\alpha, n) + I_{2,1}(\alpha, n) \right) \qquad (17)$$

$$I_2(\alpha, n) = \frac{2}{n + d - 2 - 2\alpha} I_{2,1}(\alpha, n) - \frac{n + 2d - 4 - 2\alpha}{n + d - 2 - 2\alpha} \frac{1}{q^2} I_2(\alpha - 1, n), \qquad (18)$$

where the inhomogeneous terms are

$$I_{11}(\alpha, n) = \quad\text{(diagram)}\quad - \frac{1}{q^2}\quad\text{(diagram)} \tag{19}$$

$$I_{21}(\alpha, n) = \frac{1}{q^2}\quad\text{(diagram)}\quad - \quad\text{(diagram)} \tag{20}$$

It can be seen that the inhomogeneous terms in the FRs (17) and (18), i.e., $I_{11}(\alpha, n)$ and $I_{21}(\alpha, n)$, are combinations of loops and chains, and thus, they are calculated according to the rules (4) and (8).

We note that, for massless two-point FIs, the subject of the study is the so-called coefficient functions, i.e., $C_i(\alpha, n)$ and $C_{i,1}(\alpha, n)$ $(i = 1, 2)$ for the diagrams under consideration $I_i(\alpha, n)$ and $I_{i,1}(\alpha, n)$ can be represented as follows

$$I_i(\alpha, n) = N_d \, C_i(\alpha, n) \, \frac{q^{\mu_1 \mu_2 \mu_3 \dots \mu_n}}{q^{2(\alpha + 2\varepsilon)}}, \quad I_{i,1}(\alpha, n) = N_d \, C_{i,1}(\alpha, n) \, \frac{q^{\mu_1 \mu_2 \mu_3 \dots \mu_n}}{q^{2(\alpha + 2\varepsilon)}}. \tag{21}$$

The result (21) corresponds to the fact that we are considering two-loop FIs. In general, the L-loop FI $I_L(\alpha_1, \alpha_2, \alpha_3, ..., \alpha_N, n)$ containing propagators with indices α_i $(i = 1, 2, 3, ..., N)$ and one TP of momenta, can be represented as

$$I_L(\alpha_1, \alpha_2, \alpha_3, ..., \alpha_N, n) = N_d \, C_L(\alpha_1, \alpha_2, \alpha_3, ..., \alpha_N, n) \, \frac{q^{\mu_1 \mu_2 \mu_3 \dots \mu_n}}{q^{2(\overline{\alpha} - d/2*(L\varepsilon))}}. \tag{22}$$

where $\overline{\alpha} = \sum_1^N \alpha_i$.

The coefficient functions $C_i(\alpha, n)$ and $C_{i,1}(\alpha, n)$ can be directly found from the rules (4) and (8). They have the form:

$$C_{1,1}(\alpha, n) = A(2, 1)\Big(A^{0,n}(1, \alpha) - A^{0,n}(1, \alpha + \varepsilon)\Big), \tag{23}$$

$$C_{2,1}(\alpha, n) = A^{0,n}(2, \alpha - 1)A^{0,n}(1, \alpha + \varepsilon) - A^{0,n}(1, \alpha)A^{0,n}(2, \alpha + \varepsilon), \tag{24}$$

where

$$A(\alpha_1, \alpha_2) = A^{0,0}(\alpha_1, \alpha_2). \tag{25}$$

and the result for $A^{n,m}(\alpha_1, \alpha_2)$ is shown in Equation (7). Thus, the coefficient functions $C_{i,1}(\alpha, n)$ and $C_{i,1}(\alpha, n)$ $(i = 1, 2)$ are represented as combinations of Γ-functions.

3.1. $I_1(0, n)$ and $I_2(0, n)$

The FIs $I_1(0, n)$ and $I_2(0, n)$ can be considered boundary conditions for the FRs (17) and (18). Moreover, in a sense, they can be obtained using Equations (4) and (8) but with the additional resummation.

Indeed, expanding in the cases of $I_1(0, n)$ and $I_2(0, n)$, the corresponding momentum products as follows:

$$\prod_{i=1}^{n} (q - k_2)^{\mu_i} = \sum_{k=0}^{n} C_n^k (-1)^k \prod_{i=1}^{k} k_2^{\mu_i} \prod_{j=1}^{n-k} q^{\mu_j} \qquad \text{for } I_1(0, n), \qquad (26)$$

$$\prod_{i=1}^{n} (k_1 - k_2)^{\mu_i} = \sum_{k=0}^{n} C_n^k (-1)^k \prod_{i=1}^{k} k_2^{\mu_i} \prod_{j=1}^{n-k} k_1^{\mu_j} \qquad \text{for } I_2(0, n), \qquad (27)$$

we found the results of $I_1(0, n)$ and $I_2(0, n)$ which can be represented as

$$I_1(0, n) = \sum_{k=0}^{n} C_n^k (-1)^k \prod_{j=1}^{n-k} q^{\mu_j} \, \bar{I}_1(0, k) \qquad (28)$$

$$I_2(0, n) = \sum_{k=0}^{n} C_n^k (-1)^k \, \bar{I}_2(n - k, k) \qquad (29)$$

where

$$\bar{I}_1(0, k) = \qquad\qquad , \qquad \bar{I}_2(n - k, k) = \qquad\qquad . \qquad (30)$$

Thus, the FIs $I_1(0, n)$ and $I_2(0, n)$ are combinations of loops and chains, and thus their coefficient functions can be found using the rules (4) and (8). So, we have for $C_1(0, n)$ and $C_2(0, n)$:

$$C_1(0, n) = \sum_{k=0}^{n} C_n^k (-1)^k A^{0,k}(1, 1) A^{0,k}(1, 1 + \varepsilon), \qquad (31)$$

$$C_2(0, n) = \sum_{k=0}^{n} C_n^k (-1)^k A^{0,k}(1, 1) A^{0,n-k}(1, 1). \qquad (32)$$

As noted at the beginning of Section 3.1, the results for $C_i(0, n)$ ($i = 1, 2$) are very important for obtaining the results of $C_i(m, n)$ for any m values using Equations (17) and (18) for $\alpha = m$. However, to calculate $C_i(0, n)$, the additional summation must be performed (see Equations (31) and (32)), the exact calculation of which can be found in [63]. Here, we only present the final results for $C_i(0, n)$ ($i = 1, 2$):

$$2n C_1(0, n - 1) = \hat{N}_2 \left[\frac{1}{\varepsilon^2} S_1(n) + \frac{1}{2\varepsilon} \left(3 S_1^2(n) + 7 S_2(n) \right) \right.$$

$$\left. + \frac{7}{6} S_1^3(n) + \frac{19}{2} S_1(n) S_2(n) + \frac{37}{3} S_3(n) - 4 S_{2,1}(n) \right], \qquad (33)$$

$$n(n + 1) C_2(0, n - 1) = (1 - (-1)^n) \hat{N}_1 \left[\frac{1}{\varepsilon^2} + \frac{2}{\varepsilon} \left(S_1(n) + \frac{1}{n + 1} \right) \right.$$

$$\left. + 2 S_1^2(n) + 4 S_2(n) + 2 S_{-2}(n) + 8 \frac{S_1(n)}{n + 1} + \frac{16}{(n + 1)^2} \right]. \qquad (34)$$

where

$$S_{\pm i}(n) = \sum_{m=1}^{n} \frac{(\pm 1)^m}{m^i}, \quad S_{\pm i,j}(n) = \sum_{m=1}^{n} \frac{(\pm 1)^m}{m^i} S_{\pm j}(m), \qquad (35)$$

$\zeta(n) = S_n(\infty)$—Euler zeta-function and N_1 and N_2 are normalization factors.

The factor N_2 is

$$\hat{N}_2 = \Gamma^2(1+\varepsilon)K_1K_2, \quad K_1 = \frac{\Gamma^2(1-\varepsilon)}{\Gamma(1-2\varepsilon)}, \quad K_2 = \frac{\Gamma(1-\varepsilon)\Gamma(1-2\varepsilon)\Gamma(1+2\varepsilon)}{\Gamma^2(1+\varepsilon)\Gamma(1-3\varepsilon)} \tag{36}$$

Since $K_2/K_1 \sim O(\varepsilon^3)$, it can be replaced by the factor $\hat{N}_1$

$$\hat{N}_1 = \Gamma^2(1+\varepsilon)\, K_1^2\,. \tag{37}$$

It is possible to add the factor $\hat{N}_1$ to the definition of μ_g^2-scale of g-scheme [91], which is related with the usual $\overline{MS}$ one as $\mu_g^2 = K_1\mu_{\overline{MS}}^2$ (see discussions in Ref. [92]).

3.2. $I_1(1,n)$ and $I_2(1,n)$

Now, we calculate the cases $I_1(1,n)$ and $I_2(1,n)$, which are very important for future studies. Indeed, we see that the FIs are finite and the corresponding $C_{j,1}(1,n)$ ($j=1,2$) have very compact form. Indeed,

$$C_{1,1}(1,n) = -\frac{1}{2\varepsilon^2}\left[2\hat{N}_1\frac{B(n+1,-1,-2)}{n+1-2\varepsilon} - \hat{N}_2\frac{B(n+1,-2,-3)}{n+1-3\varepsilon}\right], \tag{38}$$

$$C_{2,1}(1,n) = -\frac{\hat{N}_2}{2\varepsilon^2}\frac{B(n+1,-1,-3)}{n+1-2\varepsilon}, \tag{39}$$

where

$$B(n+1,a_1,a_2) = \frac{\Gamma(n+1+a_1\varepsilon)\Gamma(1+a_2\varepsilon)}{\Gamma(1+a_1\varepsilon)\Gamma(n+1+a_2\varepsilon)}\,. \tag{40}$$

Expanding Γ-functions as

$$\frac{\Gamma(n+1+a\varepsilon)}{n!\Gamma(1+a\varepsilon)} = exp\left[-\sum_{m=1}^{\infty}\frac{(-a\varepsilon)^m}{m}S_m(n)\right], \tag{41}$$

$$\Gamma(1+a\varepsilon) = exp\left[-\gamma a\varepsilon + \sum_{m=1}^{\infty}\frac{(-a\varepsilon)^m}{m}\zeta_m\right], \tag{42}$$

with the Euler's constant γ, we obtain ($a_\pm = a_1 \pm a_2$)

$$B(n+1,a_1,a_2) = exp\left[-\sum_{m=1}^{\infty}\frac{(-\varepsilon)^m}{m}\left[a_1^m - a_2^m\right]S_m(n)\right] = 1 + a_-\varepsilon S_1(n) + \frac{\varepsilon^2}{2}\left[a_-^2 S_1^2(n) - a_-a_+ S_2(n)\right]$$

$$+\frac{\varepsilon^3}{3!}\left[a_-^3 S_1^3(n) - 3a_-^2 a_+ S_1(n)S_2(n) + 2(a_1^3 - a_2^3)S_3(n)\right] + O(\varepsilon^4)\,. \tag{43}$$

With the evaluation of the results (38) and (39), we see that all singularities are canceled and the final results are (δ_n^m for the Kronecker symbol: $\delta_n^n = 1$ and $\delta_n^m = 0$ for $n \neq m$)

$$(n+1)C_1(1,n) = S_3(n) + S_1(n)S_2(n) - S_{2,1}(n) + 6\zeta_3 + O(\varepsilon), \tag{44}$$

$$(n+1)C_2(1,n) = (1+(-1)^n)\left(3\delta_n^0\zeta_3 - (1-\delta_n^0)\frac{2S_{-2}(n)}{n}\right) + O(\varepsilon)\,, \tag{45}$$

where we use the condition $C_1(1, n=0) = 6\zeta_3$, since $C_2(1, n=0) = C_1(1, n=0)$. (The result $C_1(1, n=0) = 6\zeta_3$ can be directly obtained from Equation (45) using an analytic continuation of $S_{-2}(n)$ (see Appendix A)).

The results (44) and (45) are the real example of the coefficient functions in DIS structure functions (see, e.g., Refs. [78,79,93]).

4. Examples of the Calculation of Four-Point Massless FIs

In the previous Section 3, we considered the basic FIs $I_1(\alpha, n)$ and $I_1(\alpha, n)$ with $\alpha = 0$ and $\alpha = 1$.

Here, we study the expansion coefficients of scalar FIs (which we call the FI "moments"), arising in the investigations of forward elastic scattering. These moments are extracted from the initial FIs with the help of the method of "projectors" [94–97], the basic properties of which are considered in Appendix B.

4.1. FIs $I_1(n+1, n)$ and $I_2(n+1, n)$

Firstly, we consider the two simplest FIs: $J_1(\alpha = 1, q, p)$ and $J_2(\alpha = 1, q, p)$, shown in Figure 2. As already discussed above, using the "projectors" method (see Appendix B), it is possible to introduce the so-called moments $J_i(\alpha = 1, n)$ $(i = 1, 2)$. The moments of the FIs shown in Figure 2 are represented by the FIs in Equation (16) for $\alpha = n + 1$, i.e., $J_i(\alpha = 1, n) = I_i(n + 1, n)$.
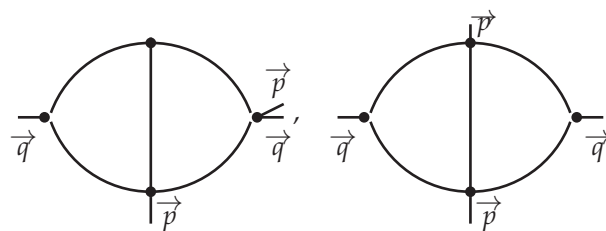

Figure 2. The simplest four-point FIs: $J_1(\alpha = 1, q, p)$ and $J_2(\alpha = 1, q, p)$.

To calculate the FIs, it is convenient to apply the Fourier transforms [16]

$$\int d^d p \, e^{ipx} \, \frac{1}{p^{2\alpha}} = 2^{2\tilde{\alpha}} \, \pi^{d/2} \, a_0(\alpha) \, \frac{1}{x^{2\tilde{\alpha}}} \, , \quad \left(\tilde{\alpha} = \frac{d}{2} - \alpha, \text{see Equation (7)}\right), \tag{46}$$

$$\int d^d p \, e^{ipx} \, \frac{p^{\mu_1} p^{\mu_2} p^{\mu_3} ... p^{\mu_n}}{p^{2(\alpha+n)}} = (-i)^n \, 2^{2\tilde{\alpha}} \, \pi^{d/2} \, a_n(\alpha+n) \, \frac{x^{\mu_1} x^{\mu_2} x^{\mu_3} ... x^{\mu_n}}{x^{2\tilde{\alpha}}} + ... \, , \tag{47}$$

where the symbol "..." marks the neglected terms of the order $g^{\mu_i \mu_j}$.

The Fourier transform (46) is the usual one (see, e.g., the recent review [16] and discussion therein) but the Fourier transform (47) can be obtained from Equation (46) using the projector $\partial^{\mu_1}/(\partial x)^{\mu_1}...\partial^{\mu_n}/(\partial x)^{\mu_n}$.

To show its effectiveness, it is possible to study more complex FIs $I_i(\alpha + n, n)$ $(i = 1, 2)$ which have coefficient functions $C_i(\alpha + n, n)$

$$I_i(\alpha + n, n) = N_d \, C_i(\alpha + n, n) \, \frac{q^{\mu_1 \mu_2 \mu_3 ... \mu_n}}{q^{2(\alpha+n+2\varepsilon)}} \, , \tag{48}$$

which are similar to Equation (21).

Applying the above Fourier transforms to the l.h.s., we obtain the following FIs in the x-space:
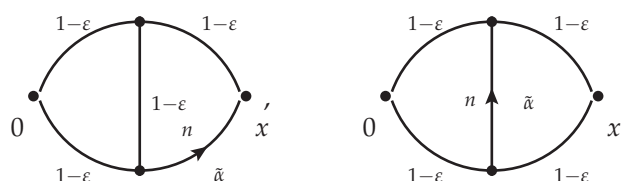
If we replace x and all internal coordinates with the momentum q and the corresponding internal momenta, we obtain equivalent diagrams in momentum space. We call them

$\overline{I}_i(\tilde{\alpha}, n)$. We call such a replacement a "dual transformation" (see discussion in [16]) and denote as $\stackrel{d}{=}$. So, we obtain

We denote the coefficient functions of the last FIs as $\overline{C}_i(\tilde{\alpha}, n)$, i.e.,

$$\overline{I}_i(\tilde{\alpha}, n) = N_d \, \overline{C}_i(\tilde{\alpha}, n) \, \frac{q^{\mu_1 \mu_2 \mu_3 \dots \mu_n}}{q^{2(\tilde{\alpha} - 2\varepsilon)}} \, . \tag{49}$$

Performing Fourier transforms for both parts of Equation (48) (see Ref. [16]), we obtain the relations between the coefficient functions $C_i(\alpha + n, n)$ and $\overline{C}_i(\tilde{\alpha}, n)$ in the following form:
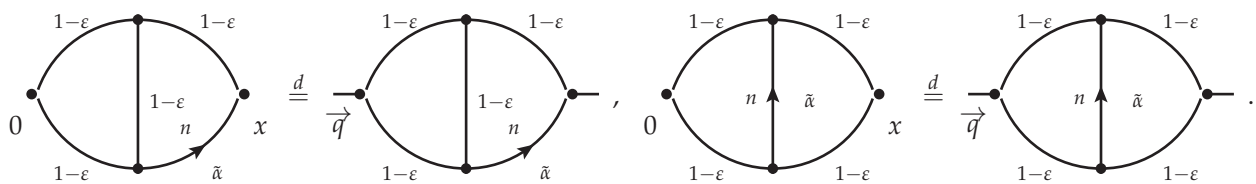
$$C_i(\alpha + n, n) = K(\alpha + n, n) \, \overline{C}_i(\tilde{\alpha}, n) \, , \tag{50}$$

where

$$K(\alpha + n, n) = \frac{a_0^4(1) a_n(\alpha + n)}{a_n(\alpha + n + 2\varepsilon)} = \frac{\Gamma^4(1 - \varepsilon)\Gamma(\tilde{\alpha})\Gamma(\alpha + n + 2\varepsilon)}{\Gamma(\alpha + n)\Gamma(\tilde{\alpha} - 2\varepsilon)} \, . \tag{51}$$

Now, we return to the case $\alpha = 1$, then

$$\overline{C}_i(1 - \varepsilon, n) = C_i(1, n) + 0(\varepsilon^0), \quad K(n + 1, n) = \frac{\Gamma^5(1 - \varepsilon)\Gamma(n + 1 + 2\varepsilon)}{n!\Gamma(1 - 3\varepsilon)} = 1 + 0(\varepsilon^0) \, . \tag{52}$$

So, we see from Equation (50) that

$$C_i(n + 1, n) = C_i(1, n) + O(\varepsilon) \, . \tag{53}$$

i.e.,

$$(n + 1)C_1(n + 1, n) = S_3(n) + S_1(n)S_2(n) - S_{2,1}(n) + 6\zeta_3 + O(\varepsilon), \tag{54}$$

$$(n + 1)C_2(n + 1, n) = (1 + (-1)^n)\left(3\delta_n^0 \zeta_3 - (1 - \delta_n^0)\frac{2S_{-2}(n)}{n} + O(\varepsilon)\right). \tag{55}$$

4.2. FIs $I_1(n + 2, n)$ and $I_2(n + 2, n)$

Now, we consider the more complicated FIs $\overline{J}_1(\alpha = 1, q, p)$ and $\overline{J}_2(\alpha = 1, q, p)$ shown in Figure 3.
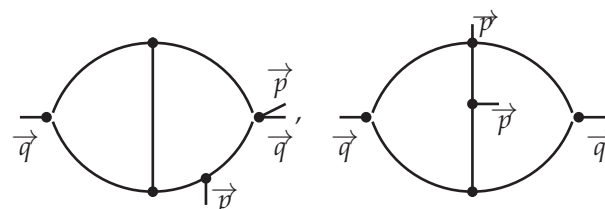
Figure 3. The FIs $\overline{J}_1(\alpha = 1, q, p)$ and $\overline{J}_2(\alpha = 1, q, p)$.

Their moments $\overline{J}_i(\alpha = 1, n)$ $(i = 1, 2)$ are equal to the FIs in Equation (16) with $\alpha = n + 2$, i.e., to $I_i(n + 2, n)$. Their coefficient functions $C_i(n + 2, n)$ $(i = 1, 2)$ can be expressed in terms of the $C_i(n + 1, n)$ given in Equations (54) and (55) and $C_{i1}(n + 2, n)$ given in Equations (23) and (24) with $\alpha = n + 2$.

Performing calculations, we obtain $C_{11}(1, n)$ and $C_{21}(1, n)$ in the following form

$$\frac{C_{11}(n+2,n)}{1/(2\varepsilon^2)} = 2\hat{N}_1 \frac{B(n+1,1,0)}{n+1} - \hat{N}_2 \frac{B(n+1,2,1)}{n+1+\varepsilon} = 2\hat{N}_1 \frac{B(n+2,1,0)}{n+1+\varepsilon} - \hat{N}_2 \frac{B(n+2,2,1)}{n+1+2\varepsilon}, \tag{56}$$

$$\frac{C_{2,1}(n+2,n)}{\hat{N}_2/(2\varepsilon^2)} = \frac{B(n+1,1,0)}{n+1+\varepsilon} B(n+1,2,1) - 3\frac{B(n+1,1,0)}{n+1} B(n+2,2,1), \tag{57}$$

where the normalizations $\hat{N}_1$ and $\hat{N}_2$ and the factors K_1 and K_2 are given in Equations (37) and (36), respectively.

Evaluating the r.h.s. of Equations (56) and (57), after some algebra, we have obtain the final results as

$$n\frac{C_1(n+1,n-1)}{\hat{N}_2} = \frac{1}{2\varepsilon^2} S_1(n) + \frac{1}{4\varepsilon}\left[3S_1^2(n) - 5S_2(n)\right] + \frac{7}{12} S_1^3(n)$$
$$-\frac{5}{4} S_1(n)S_2(n) + \frac{19}{6} S_3(n) - 2S_{2,1}(n) - \frac{S_1(n)}{n^2}, \tag{58}$$

$$n(n+1)\frac{C_2(n+1,n-1)}{\hat{N}_2} = (1-(-1)^n)\left(\frac{1}{\varepsilon^2} + \frac{2}{\varepsilon}\left[S_1(n) - \frac{1}{n+1}\right]\right.$$
$$\left.+2S_1^2(n) - 2S_2(n) - 4\frac{S_1(n)}{n+1} + \frac{1}{(n+1)^2}\right), \tag{59}$$

where we added the extra factor $(1-(-1)^n)/2$ to the coefficient function $C_2(n+1,n-1)$. The demonstration of even more complicated examples can be seen in Refs. [20–22].

We note that, for FIs containing several propagators depending on the momentum p (see, e.g., $\hat{J}_1(\alpha,\beta,q,p)$ in Appendix B), their moments contain the sum of two-point FIs (see, for example, the moment $\hat{J}_1(\alpha,\beta,n)$ in Appendix B). Calculating the moments of such a type is a much more difficult task than $I_i(n+1,n)$ and $I_i(n+2,n)$ with the $(i = 1,2)$ considered above. However, as it was shown in Ref. [22], it is almost always possible to split in the contributions the complicated integrals and complicated series. Moreover, ε-singularities are only contained in the simplest parts, which can usually be summed up in all orders in ε.

5. kR'-Operation

The calculation of massless FIs is the most important procedure for calculating the critical parameters of models and theories, such as the anomalous dimensions of fields and operators, as well as β-functions. One of the most convenient calculation recipes is that of the Bogolyubov–Parasyuk–Hepp–Zimmerman (BPHZ) R-operation [98–100], which sequentially extracts all FI singularities. Formally, it has the following form

$$R[FI] = FI - kR'[FI], \tag{60}$$

where kR' is the operation that takes into account all the singularities of the FI subgraphs, with the exception of the singularities of the FI itself. The very important property of the kR'-operation is the independence of the results of its application from the external momenta and masses. The independence is the basis of the so-called infra-red rearrangement approach [101] (as can also be seen in Ref. [102–104]), which gives a possibility to only study FIs with the minimum possible set of masses and external momenta. We note that such neglecting masses and momenta should not lead to an appearance of infrared singularities. The possibility to delete and modify external momenta is widely used (see, e.g., [105] and the discussions therein). We will try to show this in our examples below, where we take a detailed look at the computation of singular structures up to five-loop FIs that contribute to the β-function of the φ^4 model.

To demonstrate the opportunities of the kR'-operation, it is useful to start with one-loop and two-loop FIs.

One loop. Putting $\alpha_1 = \alpha_2 = 1$ in Equation (8), we obtain

$$\text{[diagram]} = N_d\, A(1,1)\, \frac{\mu^{2\varepsilon}}{q^{2\varepsilon}} = N_d\, \frac{\Gamma^2(1-\varepsilon)}{\varepsilon\Gamma(2-2\varepsilon)}\, \frac{\overline{\mu}^{2\varepsilon}}{q^{2\varepsilon}}, \tag{61}$$

where N_d is given in Equation (6) and $\overline{\mu}$ is the renormalization scale in the $\overline{MS}$-scheme, defined as

$$\overline{\mu}^{2\varepsilon} = \mu^{2\varepsilon}\, (4\pi)^\varepsilon\, \Gamma(1+\varepsilon). \tag{62}$$

By definition, kR' is an operation, which is equal to k-operation in the one-loop case, since there are no subgraphs, i.e.,

$$k\left[\;\text{[diagram]}\;\right] = N_4\, \frac{1}{\varepsilon}, \quad N_4 = N_{d=4} = \frac{1}{(4\pi)^2}, \tag{63}$$

which, of course, does not depend on q^2.

Two loops. Now, we consider the following FI

$$\text{[diagram]} = N_d^2\, A(1,1)\, A(1,1+\varepsilon)\, \frac{\mu^{4\varepsilon}}{q^{4\varepsilon}} = \frac{N_d^2}{2\varepsilon^2(1-2\varepsilon)}\, \frac{\Gamma^3(1-\varepsilon)\Gamma(1+2\varepsilon)}{\Gamma(2-3\varepsilon)\Gamma^2(1+\varepsilon)}\, \frac{\overline{\mu}^{2\varepsilon}}{q^{2\varepsilon}}. \tag{64}$$

As already mentioned, the R'-operation extracts the singularities of subgraphs. In the case under consideration, we have a singular inner loop, the singularity of which is shown above in Equation (63). Thus, the R'-operation of the considered two-loop FI has the form

$$R'\left[\;\text{[diagram]}\;\right] = \text{[diagram]} - N_4\, \frac{1}{\varepsilon}\; \text{[diagram]}. \tag{65}$$

Evaluating diagrams in the r.h.s. and taking their singular parts (by the k-operation), we obtain

$$kR'\left[\;\text{[diagram]}\;\right] = k\left[\;\text{[diagram]} - N_4\, \frac{1}{\varepsilon}\; \text{[diagram]}\;\right] \tag{66}$$

$$= N_4^2\left[\frac{1}{2\varepsilon^2}\left(1 + (5+2L)\varepsilon\right) - \frac{1}{\varepsilon^2}\left(1 + (2+L)\varepsilon\right)\right] = N_4^2\left[-\frac{1}{2\varepsilon^2} + \frac{1}{2\varepsilon}\right],$$

where

$$L = \ln\left(\frac{\overline{\mu}^2}{q^2}\right). \tag{67}$$

As we can see, the result is q^2-independent, which is due to the local renormalization properties.

Three and four loops. To find three- and four-loop corrections to the β-function of the φ^4 model, it is necessary, in particular, to calculate the singular parts of the following vertex FIs:

$$\text{(68)}$$
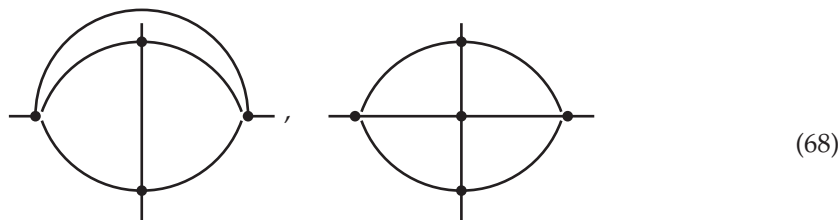
For the first diagram, we have

$$k\left[\text{(diagram)} \right] = \frac{N_4}{3\varepsilon} \text{ Finite}\left[\text{(diagram)} \right] = \frac{2N_4^3}{\varepsilon}\zeta_3, \quad \text{(69)}$$

where we used the result $C_2(n+1, n)$ in Equation (55) for $n = 0$.

We note that, for $\alpha_i = 1 + a_i\varepsilon$, there is the following result (beyond $O(\varepsilon^2)$, the coefficients of the expansion can be found in [15,90].).

$$= \frac{\hat{N}_d^2}{(q^2)^{1+(a+2)\varepsilon}} \frac{1}{1-2\varepsilon}\left[6\zeta_3 + 9\zeta_4\varepsilon + \left(42 + \sum_{i=1}^{2}A_{2,i}\right)\zeta_5\varepsilon^2 + O(\varepsilon^3)\right], \quad \text{(70)}$$

where

$$\hat{N}_d = N_d\,\Gamma(1+\varepsilon), \quad a = \textstyle\sum_{i=1}^{5}a_i, \quad A_{2,1} = 30\overline{A}_1 + 45a_5, \quad \overline{A}_n = \textstyle\sum_{i=1}^{4}a_i^n, \tag{71}$$

$$A_{2,2} = 10\overline{A}_2 + 45a_5^2 + 15\overline{A}_1 a_5 + 10\left(a_1 a_2 + a_3 a_4 + a_1 a_4 + a_2 a_3\right) + 5\left(a_1 a_3 + a_2 a_4\right).$$

The result (70) was obtained using the IBP relation (14) and transformation rules (see, e.g., [15] and the references therein). Indeed, for the case $\alpha_2 = \alpha_4 = \alpha_5 = 1$, we have from Equation (14)

$$\text{(72)}$$

$$+\alpha_4\left[\alpha_1 \leftrightarrow \alpha_4\right] = \left(\alpha_1 A(\alpha_1 + 1, \alpha_4) + \alpha_4 A(\alpha_1, \alpha_4 + 1)\right)$$
$$\times\left[A(1,1) - A(\alpha_1 + \alpha_4 - 1 + \varepsilon, 1)\right]\frac{N_d^2}{(q^2)^{\alpha_1 + \alpha_4 - 1 + 2\varepsilon}}.$$

For the second diagram in (68), we have

$$k\left[\ \ \right] = k\left[\ \underline{A} \qquad \underline{B}\ \right], \qquad (73)$$

since the singularity does not depend on the external momenta. So, we have

$$k\left[\ \ \right]_{B} = \frac{N_4}{4\varepsilon}\,\text{Finite}\left[\ \ \right] = \frac{5N_4^4}{\varepsilon}\,\zeta_5\,, \qquad (74)$$

because

$$\vec{q} = \left[20\zeta_5 + O(\varepsilon)\right]\frac{\hat{N}_d^3}{(q^2)^{1+3\varepsilon}}. \qquad (75)$$

The result (75) can be obtained as follows. Using the IBP relation for an interior triangle with the distinguished line between the top interior points, we have

$$(d-4)\ \vec{q} = 2\left[\ \ 2\ \vec{q} - 2\ \ \vec{q}\ \right] \qquad (76)$$

$$= 2N_d A(2,1)\left[\ \ 1+\varepsilon\ \vec{q} - \ 1+\varepsilon\ \vec{q}\ \right].$$

Using other IBP relations and transformation rules (see, e.g., [15] and references therein), a more accurate result can be obtained for $\alpha_i = 1 + a_i$ ($i = 1, 2, 3, ..., 7$)

$$\begin{array}{c}\alpha_2 \\ \alpha_1 \quad \alpha_3 \\ \alpha_6 \ \alpha_7 \\ \alpha_5 \quad \alpha_4 \ \vec{q}\end{array} = \frac{\hat{N}_d^3}{(q^2)^{1+a+3\varepsilon}}\frac{1}{1-2\varepsilon}\left[20\zeta_5 + \left(50\zeta_6 + (44 - a_{4567})\zeta_3^2\right)\varepsilon + O(\varepsilon^2)\right], \qquad (77)$$

where $a_{4567} = \sum_{i=4}^{7} a_i$ and $a = \sum_{i=1}^{7} a_i$.

Five Loop Corrections in the φ^4 Model

We apply the method described above to the calculation of five-loop singularities in the φ^4 model. In this regard, let us recall that the five-loop corrections to anomalous dimensions and the β-function in this model in the scheme $\overline{MS}$ were calculated a long time ago in [30]. For a complete calculation, it was necessary to calculate about 120 diagrams. The results for all but four were analytically found using the IBP procedure. For the four

most complex diagrams, the application of the decomposition of one of the propagators into Gegenbauer polynomials led to results in the form of a triple infinite convergent series. The computer summation of the series allowed the authors to achieve good accuracy. However, it was desirable to obtain an analytic assessment of these contributions, which was performed by Kazakov (see Refs. [13,90]). To show the possibilities of the methods discussed above, we present the calculation of two of these complex FIs, which have the following form

$$(78)$$

First FI. Calculating the first FI with an accuracy of $O(\varepsilon^{-1})$ is equal to calculating the diagram

$$(79)$$

with an accuracy of $O(\varepsilon)$. Using the IBP procedure to the left triangle with the vertical distinguished line, we have the following relation:

$$(80)$$

The first diagram in the r.h.s. is the product of one-loop and two-lop FIs that are already considered above. To evaluate the second diagram, the IBP procedure is applied to the left triangle with the upper distinguished line to the diagram in Equation (75). We have

$$(81)$$

Taking this equation together with Equation (76), we obtain the following

$$(82)$$

Then, plugging this result into the r.h.s. of Equation (80) and calculating the one-loop diagram, we have for the r.h.s.:

$$\frac{2N_d}{q^2} A(2,1) \left[-\!\!\bigcirc\!\!\underset{\overrightarrow{q}}{}\; q^{2\varepsilon} + 3 \;-\!\!\bigcirc\!\!\underset{\overrightarrow{q}}{1+\varepsilon}\; - 4 \;-\!\!\underset{1+\varepsilon}{\bigcirc}\!\!\underset{\overrightarrow{q}}{} \right]. \tag{83}$$

Evaluating these two-loop master integrals using the result provided by Equation (70), we obtain the results of the FI in Equation (79) with the accuracy $O(\varepsilon^2)$:

$$-\!\!\bigcirc\!\!- \;=\; \frac{N_d^3}{(q^2)^{2+3\varepsilon}} \frac{1}{1-2\varepsilon} \left[20\zeta_5 + \left(50\zeta_6 + 44\zeta_3^2\right)\varepsilon + \left(317\zeta_7 + 132\zeta_4\zeta_3\right)\varepsilon^2 + O(\varepsilon^3) \right]. \tag{84}$$

Taking into account the two additional loops, we have the additional factor:

$$A(1,2+3\varepsilon)A(1,1+4\varepsilon) = -\frac{N_d^2}{20\varepsilon^2}\frac{1}{(1+3\varepsilon)(1-6\varepsilon)}\frac{\Gamma^2(1-\varepsilon)\Gamma(1-4\varepsilon)\Gamma(1+6\varepsilon)}{\Gamma(1+3\varepsilon)\Gamma(1-6\varepsilon)}. \tag{85}$$

So, the final result for the first FI in Equation (78) has the form:

$$-\!\!\bigcirc\!\!- \;=\; -\frac{\hat{N}_d^5}{(q^2)^{5\varepsilon}} \frac{1}{20(1-2\varepsilon)(1+3\varepsilon)(1-6\varepsilon)}$$

$$\times \left[\frac{20}{\varepsilon^2}\zeta_5 + \left(50\zeta_6 + 44\zeta_3^2\right)\frac{1}{\varepsilon} + 317\zeta_7 + 132\zeta_4\zeta_3 + O(\varepsilon) \right]. \tag{86}$$

Second FI. Now, consider the second FI in Equation (78). The kR'-operation of the diagram has the following form

$$kR'\left[-\!\!\bigcirc\!\!\underset{\overrightarrow{q}}{}\underset{A}{}\underset{B}{} \right] \;=\; k\left[-\!\!\bigcirc\!\!\underset{\overrightarrow{q}}{}\underset{A}{}\underset{B}{} - N_4\frac{1}{\varepsilon}\;-\!\!\underset{\overrightarrow{q}}{}\bigcirc\underset{A}{}\underset{B}{} \right], \tag{87}$$

which contains the FI itself and its counter-term containing the inner-loop singularity.

Since the r.h.s. should be q^2-independent, the external momenta can be canceled and inserted into points A and B:

$$kR'\left[-\!\!\bigcirc\!\!\underset{\overrightarrow{q}}{}\underset{A}{}\underset{B}{} \right] \;=\; k\left[\;\bigcirc\underset{A}{}\underset{B}{}\underset{\overrightarrow{q}}{} - N_4\frac{1}{\varepsilon}\;-\!\!\underset{\overrightarrow{q}}{}\bigcirc\underset{A}{}\underset{B}{} \right]. \tag{88}$$

The r.h.s. now looks like this

$$\frac{A \quad B}{\overset{\longrightarrow}{q}}\underset{}{I_4} - \frac{N_4}{\varepsilon}\frac{A \quad B}{\overset{\longrightarrow}{q}}\underset{}{I_3} = N_d\,C_4\,A(1, 1 + 4\varepsilon)\left(\frac{\mu^2}{q^2}\right)^{5\varepsilon} - N_d N_4\frac{C_3}{\varepsilon}\,A(1, 1 + 3\varepsilon)\left(\frac{\mu^2}{q^2}\right)^{4\varepsilon}, \qquad (89)$$

where integrals I_4 and I_3 are internal blocks forming the FIs in r.h.s. of Equation (88) after integrating these blocks with the propagator connecting points A and B. Due to dimensional properties, integrals I_4 and I_3 should have the form

$$\frac{A \quad B}{\overset{\longrightarrow}{q}}\underset{}{I_4} = N_d^4\,C_4\,\frac{(\mu^2)^{4\varepsilon}}{(q^2)^{1+4\varepsilon}}, \qquad \frac{A \quad B}{\overset{\longrightarrow}{q}}\underset{}{I_3} = N_d^3\,C_3\,\frac{(\mu^2)^{3\varepsilon}}{(q^2)^{1+3\varepsilon}}, \qquad (90)$$

where C_4 and C_3 are the coefficient functions of the I_4 and I_3 integrals.

So, we have that

$$kR'\left[\begin{array}{c} A \\ \overset{\longrightarrow}{q} \\ B \end{array}\right] = N_4\,\text{Sing}\left[C_4\,A(1, 1 + 4\varepsilon) - \frac{C_3}{\varepsilon}\,A(1, 1 + 3\varepsilon)\right], \qquad (91)$$

where all q^2-dependence is canceled in the r.h.s. singularities.

For FIs similar to the diagrams in r.h.s. of Equation (88), but with the index $1 - \varepsilon$ on the line between A and B, we have the following

$$kR'\left[\begin{array}{c} C \\ \overset{\longrightarrow}{q} \\ A \quad B \\ 1-\varepsilon \end{array}\right] = N_4\,\text{Sing}\left[C_4\,A(1 - \varepsilon, 1 + 4\varepsilon) - \frac{C_3}{\varepsilon}\,A(1 - \varepsilon, 1 + 3\varepsilon)\right]. \qquad (92)$$

We would like to note that, in the l.h.s., we can extract the line between points A and C, as an external line; then, we have

$$kR'\left[\begin{array}{c} C \\ \overset{\longrightarrow}{q} \\ A \quad B \\ 1-\varepsilon \end{array}\right] = k\left[\begin{array}{c} C \\ \overset{\longrightarrow}{q} \\ A \quad B \\ 1-\varepsilon \end{array} - \frac{1}{\varepsilon}\,\begin{array}{c} C \\ \overset{\longrightarrow}{q} \\ A \\ B \\ 1-\varepsilon \end{array}\right] \qquad (93)$$

and, thus,

$$kR'\left[\begin{array}{c} C \\ \overset{\longrightarrow}{q} \\ A \quad B \\ 1-\varepsilon \end{array}\right] = N_4\,\text{Sing}\left[C_{4,1}\,A(1, 1 + 3\varepsilon) - \frac{C_{3,1}}{\varepsilon}\,A(1, 1 + 2\varepsilon)\right], \qquad (94)$$

where $C_{4,1}$ and $C_{3,1}$ are the coefficient functions of the integrals $I_{4,1}$ and $I_{3,1}$, which are internal blocks that create FIs in the r.h.s. of Equation (93) after integrating these blocks with the propagator between points A and C. Due to the dimension properties, the $I_{4,1}$ and $I_{3,1}$ integrals can be represented in the form

$$\underset{\overrightarrow{q}}{\overset{A \qquad C}{\bigcirc I_{4,1}}} = N_d^4 \, C_{4,1} \frac{(\mu^2)^{4\varepsilon}}{(q^2)^{1+3\varepsilon}}, \qquad \underset{\overrightarrow{q}}{\overset{A \qquad C}{\bigcirc I_{3,1}}} = N_d^3 \, C_{3,1} \frac{(\mu^2)^{3\varepsilon}}{(q^2)^{1+2\varepsilon}}, \qquad (95)$$

because both $I_{4,1}$ and $I_{3,1}$ contain one line with the index $1 - \varepsilon$.

Now, consider an FI similar to the original one, but with lines between points A and B and points A and C having indexes $1 - \varepsilon$. Taking, as stated above, the line between points A and C as the outer one, we obtain the results

$$kR' \left[\; \underset{\overrightarrow{q}}{\overset{D}{\bigcirc}} \; \right] = N_4 \, \mathrm{Sing} \left[C_{4,1} \, A(1 - \varepsilon, 1 + 3\varepsilon) - \frac{C_{3,1}}{\varepsilon} A(1 - \varepsilon, 1 + 2\varepsilon) \right]. \qquad (96)$$

Now, we can represent the l.h.s. FI as blocks containing two lines with the index $1 - \varepsilon$ and some additional lines between D and E:

$$kR' \left[\; \underset{\overrightarrow{q}}{\overset{D}{\bigcirc}} \; \right] = \; k \left[\; \underset{\overrightarrow{q}}{\overset{D}{\bigcirc}} \; - \; \frac{1}{\varepsilon} \; \underset{\overrightarrow{q}}{\overset{D}{\bigcirc}} \; \right]$$

$$= N_d \, \mathrm{Sing} \left[C_{4,2} \, A(1, 1 + 2\varepsilon) - \frac{C_{3,2}}{\varepsilon} A(1, 1 + \varepsilon) \right], \qquad (97)$$

where $C_{4,2}$ and $C_{3,2}$ are the coefficient functions of integrals $I_{4,2}$ and $I_{3,2}$, which can be obtained from r.h.s. FIs by removing the line between D and E. Since $I_{4,2}$ and $I_{3,2}$ have two lines with index $1 - \varepsilon$, from the dimension properties, they can be represented as

$$\underset{\overrightarrow{q}}{\overset{D \qquad E}{\bigcirc I_{4,2}}} = N_d^4 \, C_{4,2} \frac{(\mu^2)^{4\varepsilon}}{(q^2)^{1+2\varepsilon}}, \qquad \underset{\overrightarrow{q}}{\overset{D \qquad E}{\bigcirc I_{3,2}}} = N_d^3 \, C_{3,2} \frac{(\mu^2)^{3\varepsilon}}{(q^2)^{1+\varepsilon}}, \qquad (98)$$

Now, consider the FI $I_{4,2}$. Integrating the inner loop, we obtain the following

$$\underset{\overrightarrow{q}}{\overset{D \qquad C \qquad E}{\bigcirc}} = N_d \, A(1,1) \; \underset{\overrightarrow{q}}{\overset{D \qquad C \qquad E}{\bigcirc}} . \qquad (99)$$

The DAC vertex in the r.h.s. FI is a unique vertex and therefore can be replaced by the corresponding triangle, as shown in Equation (12). So, we see that

$$N_d \, A(1,1) \; \underset{\overrightarrow{q}}{\overset{D \qquad C \qquad E}{\bigcirc}} = \; \underset{\overrightarrow{q}}{\overset{D \qquad C \qquad E}{\bigcirc}} \qquad (100)$$

Now, the triangle CBE in the r.h.s. FI is uniquetriangle and therefore can be replaced by the corresponding vertex according to the rule (12):

$$\text{(diagram)} = N_d\, A(1,1) \quad \text{(diagram)} \tag{101}$$

So, finally we obtain

$$\text{(diagram)} = N_d\, A(1,1) \quad \text{(diagram)} = N_d\, A(1,1)\, J_1^{(1)}\, \frac{1}{q^{2\varepsilon}}, \tag{102}$$

where the integral $J_1^{(1)}$ is table one (see Ref. [16]) (note that the results obtained in [16] are a simple recalculation of the previously obtained x-space results [8–13]. It is convenient to use the concept of so-called dual diagrams for recalculation (see, for example, Refs. [20–22] and the discussion in Section 4.1), which were obtained from the original FIs by replacing all momenta with coordinates. With such a replacement, the results themselves remain unchanged, only their graphical representation changes. As a rule, dual diagrams are used in the massless case (as can be seen in [20–22]), but sometimes they are also used for FIs with massive propagators (see, for example, [28,29,106])): $J_1^{(1)} = J_1(1,1,1,1,1,1-\varepsilon,1-\varepsilon)$. Here,

$$J_1(a_1,a_2,a_3,a_4,a_5,a_6,a_7)(q^2) = \text{(diagram)} = N_4^3\, C_1(a_1,a_2,a_3,a_4,a_5,a_6,a_7)\, \frac{(\bar{\mu}^2)^{3\varepsilon}}{(q^2)^{a-3d/2}}, \tag{103}$$

where $a = \sum_{k=1}^7 a_i$, $a_{4567} = \sum_{k=4}^7 a_i$ and

$$C_1(a_1,a_2,a_3,a_4,a_5,a_6,a_7) = \frac{1}{1-2\varepsilon}\left[20\zeta_5 + \left(50\zeta_6 + (20 + a_{4567})\zeta_3^3\right)\varepsilon + O(\varepsilon^2)\right]. \tag{104}$$

By entering short notations $C_1^{(1)} = C_1(1,1,1,1,1,1-\varepsilon,1-\varepsilon)$ and $C_1^{(0)} = C_1(1,1,1,1,1,1,1)$, it is convenient to write the following:

$$C_1^{(1)} = C_1^{(0)}\left(1 + \frac{3\zeta_3^2}{10\zeta_5}\varepsilon\right), \tag{105}$$

where

$$C_1^{(0)} = \frac{10}{1-2\varepsilon}\left[2\zeta_5 + (5\zeta_6 + 2\zeta_3^3)\varepsilon + O(\varepsilon^2)\right] \tag{106}$$

The counter-terms $I_3(q^2)$, $I_{3,1}(q^2)$ and $I_{3,2}(q^2)$ can also be expressed through $J_1(a_1,a_2,a_3,a_4,a_5,a_6,a_7)$ in the form:

$$I_{3,2}(q^2) = J_1(1,1-\varepsilon,1-\varepsilon,1,1,1,1),\ I_{3,1}(q^2) = J_1(1-\varepsilon,1,1,1,1,1,1),\ I_3(q^2) = J_1(1,1,1,1,1,1,1). \tag{107}$$

So, within the accuracy $O(\varepsilon^2)$, their coefficient functions exactly coincide:

$$C_3 = C_{3,1} + O(\varepsilon^2) = C_{3,2} + O(\varepsilon^2) = C_1^{(0)} + O(\varepsilon^2). \tag{108}$$

Taking into account the above relations and the one-loop results $A(\alpha, \beta)$, it can be shown that with an accuracy of $O(\varepsilon^2)$, the results for the four-loop coefficient functions are also the same. Indeed, we obtain

$$C_{4,1} = C_{4,2} \frac{A(1, 1+2\varepsilon)}{A(1-\varepsilon, 1+3\varepsilon)} - \frac{C_{3,1}}{\varepsilon} \frac{e^{(-L\varepsilon)}}{A(1-\varepsilon, 1+3\varepsilon)} \left[A(1, 1+\varepsilon) - A(1-\varepsilon, 1+2\varepsilon) \right] + O(\varepsilon^2),$$

$$C_4 = C_{4,1} \frac{A(1, 1+3\varepsilon)}{A(1-\varepsilon, 1+4\varepsilon)} - \frac{C_3}{\varepsilon} \frac{e^{(-L\varepsilon)}}{A(1-\varepsilon, 1+4\varepsilon)} \left[A(1, 1+2\varepsilon) - A(1-\varepsilon, 1+3\varepsilon) \right] + O(\varepsilon^2).$$
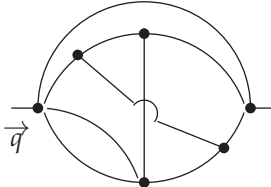
The terms $\sim C_{3,1}$ and $\sim C_3$ are suppressed and we obtain the following

$$C_4 = C_{4,1} + O(\varepsilon^2) = C_{4,2} + O(\varepsilon^2) \tag{109}$$
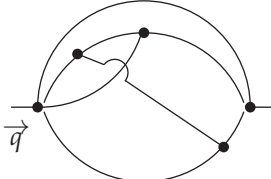
and, thus,

$$C_4 = C_1^{(1)} + O(\varepsilon^2) = C_1^{(0)} \left(1 + \frac{3\zeta_3^2}{10\zeta_5} \varepsilon \right) + O(\varepsilon^2). \tag{110}$$

So, the results for initial diagrams, as shown in the r.h.s. of Equation (87), using the r.h.s. of Equation (91), can be represented as
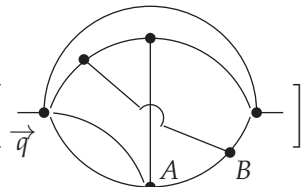

$$= N_4^5 \frac{C_1^{(1)}}{5\varepsilon^2 (1-2\varepsilon)(1-6\varepsilon)} \left(\frac{\bar{\mu}^2}{q^2} \right)^{5\varepsilon} \tag{111}$$

and
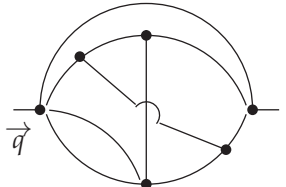
$$= N_4^4 \frac{C_1^{(0)}}{4\varepsilon^2 (1-5\varepsilon)} \left(\frac{\bar{\mu}^2}{q^2} \right)^{4\varepsilon}. \tag{112}$$

So, for the second diagram in Equation (78), we have

$$kR' \left[\; \text{} \; \right] = N_4^5 \, \text{Sing} \left[\frac{C_1^{(1)} e^{5L\varepsilon}}{5\varepsilon^2 (1-2\varepsilon)(1-6\varepsilon)} - \frac{C_1^{(0)} e^{4L\varepsilon}}{4\varepsilon^2 (1-5\varepsilon)} \right], \tag{113}$$

where the definition of L is presented in Equation (67). Taking into account the results for $C_1^{(1)}$ and $C_1^{(0)}$, given in Equations (105) and (106), respectively, we obtain the final following result:

$$kR' \left[\; \text{} \; \right] = -N_4^5 \left[\frac{\zeta_5}{\varepsilon^2} + \frac{1}{\varepsilon} \left(\frac{5}{2} \zeta_6 + \frac{17}{5} \zeta_3^2 - 5\zeta_5 \right) \right]. \tag{114}$$

The reception of this result came a long way; however, all steps are absolutely transparent. Moreover, a similar approach can be used to evaluate other FIs.

6. Calculation of Massive FIs

FIs with massive propagators are significantly more complicated objects compared to massless FIs. The basic rules for FI calculating, as already discussed in Section 2, should be supplemented with new rules containing directly massive propagators. These additional rules will be introduced now.

A propagator with the index α and mass M is graphically represented as

$$\frac{1}{(q^2 + M^2)^\alpha} = \underset{\overrightarrow{q} \qquad \alpha}{\overset{M}{\rule{3cm}{0.4pt}}} \, , \tag{115}$$

The following useful formulas exist.

A. The product of propagators with indices α_1 and α_2 and with the same mass M (i.e., the chain of two massive propagators with the same mass) is equivalent to a new propagator with index $\alpha = \alpha_1 + \alpha_2$ and mass M:

$$\frac{1}{(q^2 + M^2)^{\alpha_1}} \frac{1}{(q^2 + M^2)^{\alpha_2}} = \frac{1}{(q^2 + M^2)^{(\alpha_1 + \alpha_2)}} \, ,$$

or graphically

$$\underset{\overrightarrow{q} \quad \alpha_1 \qquad \alpha_2}{\overset{M \qquad\quad M}{\rule{3cm}{0.4pt}}} = \underset{\overrightarrow{q} \quad \alpha_1 + \alpha_2}{\overset{M}{\rule{3cm}{0.4pt}}} . \tag{116}$$

B. Massive tadpole is exactly integrated:

$$\int \frac{Dk}{k^{2\alpha_1}(k^2 + M^2)^{\alpha_2}} = N_d \frac{R(\alpha_1, \alpha_2)}{M^{2(\alpha_1 + \alpha_2 - d/2)}}$$

where

$$R(\alpha, \beta) = \frac{\Gamma(d/2 - \alpha_1)\Gamma(\alpha_1 + \alpha_2 - d/2)}{\Gamma(d/2)\Gamma(\alpha_2)} . \tag{117}$$

C. The result of calculating the FI containing two massive propagators (i.e., a loop) with masses M_1 and M_2 and indices α_1 and α_2 can be represented as a $_2F_1$-hypergeometric function that can be obtained in various ways, for example, by the Feynman-parameter method. However, using this approach, it is very useful to represent the loop as a one-fold integral of the new propagator with an 'effective mass' μ [23–27,62,107–110]:

$$\times \int \frac{Dk}{[(q - k)^2 + M_1^2]^{\alpha_1}[k^2 + M_2^2]^{\alpha_2}}$$

$$= N_d \frac{\Gamma(\alpha_1 + \alpha_2 - d/2)}{\Gamma(\alpha_1)\Gamma(\alpha_2)} \int_0^1 \frac{ds \, s^{\alpha_1 - 1}(1 - s)^{\alpha_2 - 1}}{[s(1 - s)q^2 + M_1^2 s + M_2^2(1 - s)]^{\alpha_1 + \alpha_2 - d/2}}$$

$$= N_d \frac{\Gamma(\alpha_1 + \alpha_2 - d/2)}{\Gamma(\alpha_1)\Gamma(\alpha_2)} \int_0^1 \frac{ds}{s^{1 - \tilde{\alpha}_2}(1 - s)^{1 - \tilde{\alpha}_1}} \frac{1}{[q^2 + \mu^2]^{\alpha_1 + \alpha_2 - d/2}}, \quad \left(\mu^2 = \frac{M_1^2}{1 - s} + \frac{M_2^2}{s}\right) .$$

It is convenient to also rewrite the equation graphically:

$$= N_d \frac{\Gamma(\alpha_1 + \alpha_2 - d/2)}{\Gamma(\alpha_1)\Gamma(\alpha_2)} \int_0^1 \frac{ds}{s^{1 - \tilde{\alpha}_2}(1 - s)^{1 - \tilde{\alpha}_1}} \underset{\overrightarrow{q} \quad \alpha_1 + \alpha_2 - d/2}{\overset{\mu}{\rule{3cm}{0.4pt}}} . \tag{118}$$

D. For any triangle with masses M_i ($i = 1, 2, 3$) and indices α_i, the following relation is obtained using the IBP procedure [7,19,23–27,87]

$$(d - 2\alpha_1 - \alpha_2 - \alpha_3)$$

$$= \alpha_2 \left[\quad - \left[(q_2 - q_1)^2 + M_1^2 + M_2^2 \right] \times \right.$$

$$\left. + \alpha_3 \left[\alpha_2 \leftrightarrow \alpha_3, M_2 \leftrightarrow M_3 \right] - 2M_1^2 \alpha_1 \times \right. \qquad . \tag{119}$$

By analogy with the massless case (see Equation (14)), Equation (119) can be obtained by introducing the coefficient $d = (\partial / \partial k_\mu)\,(k - q_1)^\mu$ to the subintegral expression of the triangle and using integration by parts as in Equation (15).

Also, similarly to the massless case, the line with the index α_1 enters asymmetrically, and as a result, it is distinguished. Therefore, we will call the line with the index α_1 as the "distinguished line". It is clear that there are different relationship options with different distinguished lines leading to different types of IBP relations.

7. Two-Loop On-Shall MI

Here, we consider the two-loop on-shall MI (in this section, we use the condition $q^2 = -m^2$, since Euclidean space is used)

$$I(m^2, M^2) = \qquad . \tag{120}$$

It contributes the α_s-correction to the ratio between the $\overline{MS}$ and the pole masses of the Higgs boson in the standard model.

Except in special cases, below we will not specify the masses of m and M, but rather thin and thick lines for the propagators with m and M, respectively.

Applying the IBP relation for the inner loop of the FI $I(m^2, M^2)$, we obtain

$$(d - 3)\,I(m^2, M^2) = \qquad - \qquad - (4M^2 - m^2) \qquad , \tag{121}$$

where the last integral in the r.h.s. can be represented as

$$-\frac{1}{2} \frac{\partial}{\partial M^2}\, I(m^2, M^2)\,. \tag{122}$$

Thus, Equation (121) can be represented as the DE

$$(4M^2 - m^2)\frac{1}{2}\frac{\partial}{\partial M^2}I(m^2, M^2) = (d-3)I(m^2, M^2) + J(m^2, M^2), \tag{123}$$

with the inhomogeneous term (IT)

$$J(m^2, M^2) = \quad \tag{124}$$

which contains only substantially simpler FIs. The DE solution with the boundary condition $J(m^2, M^2 \to \infty) = 0$ has the following form

$$I(M^2, m^2) = N_d^2 \bar{I}(x)\frac{(\bar{\mu}^2)^{2\varepsilon}}{(m^2)^{2\varepsilon}}, \quad J(M^2, m^2) = N_d^2 \bar{J}(x)\frac{\bar{\mu}^2}{(m^2)^{2\varepsilon}}, \tag{125}$$

$$\bar{I}(x) = -(4x-1)^{1/2-\varepsilon}\int_x^\infty \frac{2\bar{I}_1(x_1)dx_1}{(4x_1-1)^{3/2-\varepsilon}} = -\frac{(4-z)^{1/2-\varepsilon}}{z^{1/2-\varepsilon}}\int_0^z \frac{2\bar{J}(z_1)dz_1}{z_1^{1/2+\varepsilon}(4-z_1)^{(3/2-\varepsilon)}}, \tag{126}$$

where

$$x = \frac{M^2}{m^2}, \quad z = \frac{M^2}{m^2} = \frac{1}{x}. \tag{127}$$

Applying the IBP procedure for each FI included in $J(M^2, m^2)$, we obtain similar DEs for them. Solving these DEs, we obtain the following result for $\bar{J}(x)$

$$\bar{J}(z) = \left[-\frac{1}{2\varepsilon^2} + \left(a_1 - \frac{3}{2}\right)\frac{1}{\varepsilon} + a_2 + 2a_1 - \frac{9}{2} + a_1\ln z + \frac{1-z}{z}\overline{\text{Li}}_2(z) + \frac{1}{2}\ln^2 z\right], \tag{128}$$

where

$$a_1 = -\frac{\pi}{\sqrt{3}}, \quad a_2 = \frac{4}{\sqrt{3}}\text{Cl}_2\left(\frac{\pi}{3}\right) - \frac{\pi}{\sqrt{3}}\ln 3, \quad \overline{\text{Li}}_2(z) = \text{Li}_2(z) + \ln z\ln(1-z) \tag{129}$$

and $\text{Li}_2(z)$ is the dilogarithm [111] (for more complicated functions, see Ref. [112]).

$\bar{I}(x)$

To calculate the FI $\bar{I}(x)$, we need to calculate several integrals. The first integral, which contains the x-independent part of $\bar{J}(x)$, is simple:

$$\bar{I}_1(x) = (4x-1)^{1/2-\varepsilon}\int_x^\infty \frac{dx_1}{(4x_1-1)^{3/2-\varepsilon}} = \frac{1}{2(1-2\varepsilon)}. \tag{130}$$

The remaining integrals will be calculated up to $\varepsilon = 0$.

The integral $\sim \ln z$ in $\bar{J}(x)$ is convenient to calculate using the IBP procedure (the IBP procedure was used in a similar way for integral representations in a recent paper [113], where FIs containing elliptic structures were considered). how

$$\bar{I}_2(x) = (4x-1)^{1/2}\int_x^\infty \frac{dx_1}{(4x_1-1)^{3/2}}\ln\left(\frac{1}{x_1}\right) = \frac{1}{2}\left[\ln\left(\frac{1}{x}\right) - \tilde{I}(x)\right], \tag{131}$$

where (see Appendix C)

$$\tilde{I}(x) = (4x-1)^{1/2}\int_x^\infty \frac{dx_1}{x_1(4x_1-1)^{1/2}} = \frac{(4-z)^{1/2}}{z^{1/2}}\int_0^z \frac{dz_1}{z_1^{1/2}(4-x_1)^{1/2}}$$

$$= \frac{2}{t}\int_0^t \frac{dt_1}{1+t_1^2} = -\frac{1+y}{1-y}\ln y \tag{132}$$

and, thus,

$$\bar{I}_2(x) = \frac{1}{2} \left[\ln z + \frac{1+y}{1-y} \ln y \right].$$ (133)

Similarly, the integral $\sim \ln^2 z$ in $\bar{J}(x)$ is calculated as

$$\bar{I}_3(x) = (4x-1)^{1/2} \int_x^\infty \frac{dx_1}{(4x_1-1)^{3/2}} \ln^2 \left(\frac{1}{x_1} \right) = \frac{1}{2} \left[\ln^2 \left(\frac{1}{x} \right) + 2\tilde{I}_1(x) \right],$$ (134)

where (see Appendix C)

$$\tilde{I}_1(x) = (4x-1)^{1/2} \int_x^\infty \frac{dx_1}{x_1(4x_1-1)^{1/2}} \ln x_1 = -\frac{(4-z)^{1/2}}{z^{1/2}} \int_0^z \frac{dz_1}{z_1^{1/2}(4-x_1)^{1/2}} \ln z_1$$

$$= -\frac{2}{t} \int_0^t \frac{dt_1}{1+t_1^2} \ln[z_1(t_1)] = -\frac{1+y}{1-y} \int_y^1 \frac{dy_1}{y_1} \ln[z_1(y_1)].$$ (135)

The integral in r.h.s. is also calculated using the IBP procedure:

$$-\int_y^1 \frac{dy_1}{y_1} \ln[z_1(y_1)] = \ln y \ln z - \int_y^1 \frac{dy_1(1+y_1)}{y_1(1-y_1)} \ln y_1 = \ln y \ln z + \frac{1}{2} \ln^2 y + 2\mathrm{Li}_2(1-y) \equiv T_1(y),$$ (136)

and thus,

$$\tilde{I}_1(x) = \frac{1+y}{1-y} T_1(y) \quad \text{and} \quad \bar{I}_3(x) = \frac{1}{2} \ln^2 z + \frac{1+y}{1-y} T_1(y).$$ (137)

Similarly, we can calculate the term $\sim \overline{\mathrm{Li}}_2(z)$ in $\bar{J}(x)$. Indeed, we have

$$\bar{I}_4(x) = (4x-1)^{1/2} \int_x^\infty \frac{dx_1(x_1-1)}{(4x_1-1)^{3/2}} \overline{\mathrm{Li}}_2(1/x_1) = \frac{1}{2} \left[-\frac{2+z}{2z} \overline{\mathrm{Li}}_2(z) + \tilde{I}_2(x) \right],$$ (138)

where

$$\tilde{I}_2(x) = -(4x-1)^{1/2} \int_x^\infty \frac{dx_1(x_1+1/2)}{x_1(4x_1-1)^{1/2}} \frac{\partial}{\partial x_1} \overline{\mathrm{Li}}_2(1/x_1)$$

$$= \frac{(4-z)^{1/2}}{z^{1/2}} \int_0^z \frac{dz_1(2+z_1)}{2z_1^{1/2}(4-z_1)^{1/2}} \frac{\partial}{\partial z_1} \overline{\mathrm{Li}}_2(z_1)$$ (139)

Since

$$\frac{\partial}{\partial z} \overline{\mathrm{Li}}_2(z) = -\frac{\ln z}{1-z}$$ (140)

we obtain

$$\tilde{I}_2(x) = -\frac{(4-z)^{1/2}}{z^{1/2}} \int_0^z \frac{dz_1(2+z_1)}{2z_1^{1/2}(4-z_1)^{1/2}} \frac{\ln z_1}{1-z_1} = -\frac{2}{t} \int_0^t \frac{dt_1(1+3t_1^2)}{(1+t_1^2)(1-3t_1^2)} \ln[z_1(t_1)]$$

$$= \frac{1}{t} \int_0^t dt_1 \left[\frac{1}{1+t_1^2} - \frac{3}{1-3t_1^2} \right] \ln[z_1(t_1)] = -\frac{1}{2} \frac{1+y}{1-y} T_1(y) - 3\tilde{I}_{21}(x).$$ (141)

Now, we evaluate the term $\tilde{I}_{21}(x)$. Considering a simpler integral at the beginning

$$\int_0^t dt_1 \frac{1}{1-3t_1^2} = -\frac{1}{2\sqrt{3}} \ln \left(\frac{1-\sqrt{3}t}{1+\sqrt{3}t} \right),$$ (142)

we see the appearance of the new useful variable

$$\xi = \frac{1-\sqrt{3}t}{1+\sqrt{3}t}$$ (143)

Using this new variable $\tilde{\zeta}$, we have for $\tilde{I}_{21}(x)$ (see also Appendix C):

$$\tilde{I}_{21}(x) = \frac{1}{2\sqrt{3}t} \int_{\tilde{\zeta}}^{1} \frac{d\tilde{\zeta}_1}{\tilde{\zeta}_1} \ln\left(\frac{(1-\tilde{\zeta}_1)^2}{(1+\tilde{\zeta}_1+\tilde{\zeta}_1^2)} \right) \tag{144}$$

Since

$$\frac{(1-\tilde{\zeta}_1)^2}{(1+\tilde{\zeta}_1+\tilde{\zeta}_1^2)} = \frac{(1-\tilde{\zeta}_1)^3}{(1-\tilde{\zeta}_1^3)} \quad \text{and} \quad \frac{1}{\sqrt{3}t} = \frac{1+\tilde{\zeta}}{1-\tilde{\zeta}}, \tag{145}$$

we can represent the integral $\tilde{I}_{21}(x)$ as (the structure $(1+\tilde{\zeta}_1+\tilde{\zeta}_1^2)$, appearing in the integrand in Equation (144), leads to the appearance of the polylogarithms with the argument $\tilde{\zeta}^3$ (see also [62,114–119]). In general, this structure leads to the appearance of the cyclotron polylogarithms [120–122].)

$$\tilde{I}_{21}(x) = \frac{1+\tilde{\zeta}}{2(1-\tilde{\zeta})} \left[3\mathrm{Li}_2(\tilde{\zeta}) - \frac{1}{3}\mathrm{Li}_2(\tilde{\zeta}^3) - \frac{8}{3}\zeta_2 \right] \equiv \frac{1+\tilde{\zeta}}{2(1-\tilde{\zeta})} T_2(\tilde{\zeta}) \tag{146}$$

and thus,

$$\tilde{I}_2(x) = -\frac{1+y}{2(1-y)} T_1(y) - \frac{3(1+\tilde{\zeta})}{2(1-\tilde{\zeta})} T_2(\tilde{\zeta}),$$

$$\overline{I}_4(x) = -\frac{2+z}{4z}\overline{\mathrm{Li}}_2(z) - \frac{1+y}{4(1-y)} T_1(y) - \frac{3(1+\tilde{\zeta})}{4(1-\tilde{\zeta})} T_2(\tilde{\zeta}) \tag{147}$$

So, the initial FI $\overline{I}(x)$ is expressed as

$$\overline{I}(x) = \frac{1}{2}\left(\frac{1}{\varepsilon^2} + \frac{5-2a_1}{\varepsilon} + 19 - 8a_1 - 2a_2 \right) - a_1\left[\ln z + \frac{1+y}{1-y}\ln y \right] - \frac{1}{2}\ln^2 z$$

$$+\frac{2+z}{2z}\overline{\mathrm{Li}}_2(z) - \frac{1+y}{2(1-y)} T_1(y) + \frac{3(1+\tilde{\zeta})}{2(1-\tilde{\zeta})} T_2(\tilde{\zeta}). \tag{148}$$

8. Basic Massive Two-Loop FIs

The general topology of the two-loop two-point FI, which is not expressed as a combination of loops and chains, is shown in Figure 4.
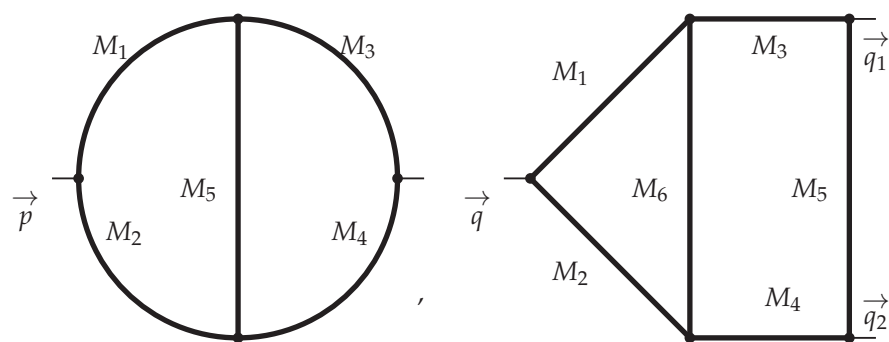

Figure 4. Two-loop two-point FI $I(M_1, M_2, M_3, M_4, M_5)$ and three-point FI $P(M_1, M_2, M_3, M_4, M_5, M_6)$ with $q_1^2 = q_2^2 = 0$.

Below, we study the two-loop two-point and three-point FIs, which are special cases of the FIs shown in Figure 4. We call these:

$$I_j = I(M_j = M \neq 0, M_p = 0, p \neq j), \quad I_{ij} = I(M_i = M_j = M \neq 0, M_p = 0, p \neq i \neq j),$$
$$I_{ijs} = I(M_i = M_j = M_s = M \neq 0, M_p = 0, p \neq i \neq j \neq s),$$
$$I_{ijst} = I(M_i = M_j = M_s = M_t = M \neq 0, M_p = 0, p \neq i \neq j \neq s \neq t), \tag{149}$$
$$P_j = P(M_j = M \neq 0, M_p = 0, p \neq j), \quad P_{ij} = P(M_i = M_j = M \neq 0, M_p = 0, p \neq i \neq j),$$
$$P_{ijs} = P(M_i = M_j = M_s = M \neq 0, M_p = 0, p \neq i \neq j \neq s),$$
$$P_{ijst} = P(M_i = M_j = M_s = M_t = M \neq 0, M_p = 0, p \neq i \neq j \neq s \neq t), \tag{150}$$

Let us repeat here once again the importance of using the IBP procedure [19,87].

First of all, its use leads to relations between various FIs and, consequently, to the need to calculate only some of them, which in some sense are independent. These independent FIs (which, of course, can be chosen completely arbitrarily) are called master integrals [61].

Using the IBP relation [19,87] for the master integrals themselves leads to DEs for them with ITs containing simpler diagrams (see [23–29]). The term 'simpler diagrams' is applicable to diagrams that usually contain fewer propagators, and sometimes they can be represented as FIs with fewer loops and with some 'effective masses' (see, for example, [62,107–110,123] and references therein). Using the IBP relation for IT diagrams leads to new DEs for them with new ITs containing even simpler FIs ($\equiv$simpler² FIs). After repeating the procedure several times, in the last step, we obtain ITs containing mainly tadpoles, which can be easily calculated (see rule B in Section 6).

By solving the DEs in this last step, it is possible to reproduce FIs for the ITs of DEs in the previous step and so on. By repeating the procedure several times, one can obtain the results for the original FI.

8.1. Results Are in the Form of Series

Consider the integral $P_x 126$ (massless and massive propagators are shown by thin and thick lines, respectively)

$$P_{126} =$$
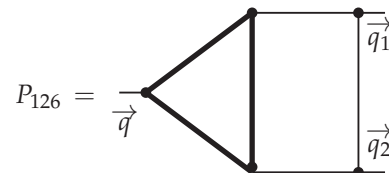
as a first example. It was calculated in Ref. [124] (see also [62,114]) and it has the series form (hereafter in Section 8 $x = q^2/m^2$):

$$P_{125} = -\frac{N_d^2 \bar{\mu}^{2\varepsilon}}{(q^2)^{2+2\varepsilon}} \sum_{n=1} \frac{(-x)^n}{2n} \frac{(n!)^2}{(2n)!} \left\{ \frac{1}{\varepsilon^2} - \frac{1}{\varepsilon} \left(S_1 + \ln x \right) + 4\bar{S}_1 S_1 - \frac{3}{2} \left(5S_1^2 + S_2 \right) - \zeta_2 \right.$$
$$\left. + \frac{2}{n} S_1 - S_1 \ln x + \frac{1}{2} \ln^2 x \right\}. \tag{151}$$

where $S_i(n)$ is defined in Equation (35) and

$$S_i = S_i(n-1), \quad \bar{S}_i = S_i(n-1) \tag{152}$$

and $\bar{\mu} = 4\pi e^{-\gamma_E} \mu$ is the $\overline{MS}$-scale and γ_E is the Euler constant.

8.2. Properties of Series

Series representations (as in Equation (151)) are convenient for calculating two-loop two-point FIs [23–29,123] and three-point FIs [62,107,108,124] with one non-zero mass. The calculation procedure using IBP relations and the construction of DEs based on it (see above) is very powerful, but rather complicated. However, there are some properties of series that either simplify calculations or sometimes allow a result to be obtained without direct calculations.

Indeed, the inverse mass decomposition of the two-loop two-point and three-point FIs with one non-zero mass can be represented as

$$
\text{FI} = \frac{N_d^2 \bar{\mu}^{2\varepsilon}}{(q^2)^{2\alpha+2\varepsilon}} \sum_{n=1} C_n (\eta x)^n \left\{ F_0(n) + \left[\ln x \, F_{1,1}(n) + \frac{1}{\varepsilon} F_{1,2}(n) \right] \right. \tag{153}
$$
$$
\left. + \left[\ln^2 x \, F_{2,1}(n) + \frac{1}{\varepsilon} \ln x \, F_{2,2}(n) + \frac{1}{\varepsilon^2} F_{2,3}(n) + \zeta(2) F_{2,4}(n) \right] + ... \right\},
$$

where $\eta = 1$ or -1 and $\alpha = 1$ and 2 for two-point and three-point FIs, respectively.

We consider two-loop FIs without the cuts of three massive particles. Thus, the results of the considered FIs should be expressed as combinations of polylogarithms. Note that the three-point FIs are only considered with independent momenta q_1 and q_2 and the conditions $q_1^2 = q_2^2 = 0$ and $(q_1 + q_2)^2 \equiv q^2 \to 0$. Moreover,

$$
C_n = \frac{(n!)^2}{(2n)!} \equiv \hat{C}_n \tag{154}
$$

for FIs having two-massive-particle-cuts ($2m$-cuts). For the FIs having only one-massive-particle-cuts (m-cuts), $C_n = 1$.

For the m-cut case, the coefficients $F_{N,k}(n)$ should have the following form

$$
F_{N,k}(n) \sim \frac{S_{\pm a, \pm b, \pm c, ...}}{n^d}, \frac{\zeta(\pm a \pm b, \pm c, ...)}{n^d}, \tag{155}
$$

where $S_{\pm a, \pm b, \pm c, ...} \equiv S_{\pm a, \pm b, \pm c, ...}(j-1)$ are harmonic sums and $\zeta(\pm a, \pm b, \pm c, ...)$ are the Euler–Zagier constants (also see Equation (35))

$$
S_{\pm a}(j) = \sum_{m=1}^{j} \frac{(\pm 1)^m}{m^a}, \quad S_{\pm a, \pm b, \pm c, ...}(j) = \sum_{m=1}^{j} \frac{(\pm 1)^m}{m^a} S_{\pm b, \pm c, ...}(m),
$$
$$
\zeta(\pm a) = \sum_{m=1}^{\infty} \frac{(\pm 1)^m}{m^a}, \quad \zeta(\pm a, \pm b, \pm c, ...) = \sum_{m=1}^{\infty} \frac{(\pm 1)^m}{m^a} S_{\pm b, \pm c, ...}(m-1). \tag{156}
$$

For the $2m$-cut case, the coefficients $F_{N,k}(n)$ are more complicated

$$
F_{N,k}(n) \sim \frac{S_{\pm a, \pm b, \pm c, ...}}{n^d}, \frac{V_{a,b,c,...}}{n^d}, \frac{W_{a,b,c,...}}{n^d}, \tag{157}
$$

where $W_{a,b,c,...} \equiv W_{a,b,c,...}(j-1)$ and $V_{a,b,c,...} \equiv V_{a,b,c,...}(j-1)$ with

$$
V_a(j) = \sum_{m=1}^{j} \frac{\hat{C}_m}{m^a}, \quad V_{a,b,c,...}(j) = \sum_{m=1}^{j} \frac{\hat{C}_m}{m^a} S_{b,c,...}(m), \tag{158}
$$

$$
W_a(j) = \sum_{m=1}^{j} \frac{\hat{C}_m^{-1}}{m^a}, \quad W_{a,b,c,...}(j) = \sum_{m=1}^{j} \frac{\hat{C}_m^{-1}}{m^a} S_{b,c,...}(m), \tag{159}
$$

The sums $\sim V_{a,b,c,...}$ and $\sim W_{a,b,c,...}$ can only appear in the $2m$-cut case. The source of their appearance is the product of two series with coefficients $C_n = 1$ and $C_n = \hat{C}_n$, respectively

8.3. Additional Examples

Consider here the two-loop two-point FIs I_1 and I_{12} calculated in [62] as additional examples

$$I_1 = \underset{\overrightarrow{q}}{\hspace{1cm}} , \quad I_{12} = \underset{\overrightarrow{q}}{\hspace{1cm}} \tag{160}$$

Their series expansions are

$$I_1 = -\frac{N_d^2 \bar{\mu}^{2\varepsilon}}{(q^2)^{1+2\varepsilon}} \sum_{n=1} \frac{(-x)^n}{n} \left\{ \frac{1}{2} \ln^2 x - \frac{2}{n} \ln x + \zeta(2) + 2S_2 - 2\frac{S_1}{n} + \frac{3}{n^2} \right\}, \tag{161}$$

$$I_{12} = -\frac{N_d^2 \bar{\mu}^{2\varepsilon}}{(q^2)^{1+2\varepsilon}} \sum_{n=1} \frac{(-x)^n}{n^2} \left\{ \frac{1}{n} + \frac{(n!)^2}{(2n)!} \left(-2\ln x - 3W_1 + \frac{2}{n} \right) \right\}. \tag{162}$$

Equation (161) shows that, for the case where the functions $F_{N,k}(n)$ in Equation (153) have the form

$$F_{N,k}(n) \sim \frac{1}{n^{3-N}}, \quad (N \geq 2), \tag{163}$$

if we introduce the following complexity level of the used sums $(\overline{\Phi} = (S, V, W))$

$$\overline{\Phi}_{\pm a} \sim \overline{\Phi}_{\pm a_1, \pm a_2} \sim \overline{\Phi}_{\pm a_1, \pm a_2, \pm a_3, \dots, \pm a_m} \sim \zeta_a \sim \frac{1}{n^a}, \quad (\sum_{i=1}^m a_i = a). \tag{164}$$

The number $3 - N$ determines the level of transcendentality (or complexity) or the weight of the coefficients $F_{N,k}(n)$ in Equation (153). This property significantly reduces the number of possible elements in $F_{N,k}(n)$. Moreover, the level of transcendentality decreases if we consider the FI singular parts and/or coefficients in the front of ζ-functions or logarithm powers. Thus, having found the simplest parts, we can predict the rest using the results already obtained as ansatz, but using them with a higher level of transcendentality.

Other two-loop two-point FIs in [62] have similar representations. They were exactly calculated by the DE method [23–29].

Now, we consider two-loop three-point FIs, P_5 and P_{12}:

$$P_5 = \underset{\overrightarrow{q}}{\hspace{1cm}} \overrightarrow{q_1} \atop \overrightarrow{q_2} , \quad P_{12} = \underset{\overrightarrow{q}}{\hspace{1cm}} \overrightarrow{q_1} \atop \overrightarrow{q_2}$$

Their series expansions are (see [62]):

$$P_5 = \frac{N_d^2 \bar{\mu}^{2\varepsilon}}{(q^2)^{2+2\varepsilon}} \sum_{n=1} \frac{x^n}{n} \left\{ -6\zeta_3 + 2S_1\zeta_2 + 6S_3 - 2S_1S_2 + 4\frac{S_2}{n} - \frac{S_1^2}{n} + 2\frac{S_1}{n^2} \right.$$
$$\left. + \left(-4S_2 + S_1^2 - 2\frac{S_1}{n} \right) \ln x + S_1 \ln^2 x \right\}, \tag{165}$$

$$P_{12} = \frac{N_d^2 \bar{\mu}^{2\varepsilon}}{(q^2)^{2+2\varepsilon}} \sum_{n=1} \frac{(-x)^n}{n^2} \frac{(n!)^2}{(2n)!} \left\{ \frac{2}{\varepsilon^2} + \frac{2}{\varepsilon} \left(S_1 - 3W_1 + \frac{1}{n} - \ln x \right) - 6W_2 - 18W_{1,1} \right.$$
$$\left. - 13S_2 + S_1^2 - 6S_1W_1 + 2\frac{S_1}{n} + \frac{2}{n^2} - 2 \left(S_1 + \frac{1}{n} \right) \ln x + \ln^2 x \right\},$$

In the last case, the coefficients $F_{N,k}(n)$ have the following form

$$F_{N,k}(n) \sim \frac{1}{n^{4-N}}, \quad (N \geq 3), \tag{166}$$

The FI P_5 (as well as FIs P_1, P_3, and P_6 in [62]) was calculated exactly by the DE method [23–29]. To calculate P_{12} (as well as for all other FIs in [62]), we used the known results of several first terms in its inverse-mass expansion in Equation (153) and the following arguments:

- When a two-loop two-point FI with a 'similar topology' (for example, I_{12} and P_{12}) has already been calculated, we consider a similar set of basic terms for the corresponding two-loop three-point FIs with a higher level of complexity.
- Let the considered FI contain the singularities and/or powers of logarithms.
  Since the coefficients in the front; the coefficients in the leading singularity; the coefficients in the front of the largest degree of the logarithm; or the coefficients in the largest ζ-function are very simple, they can often be predicted directly from the first few coefficients of the considered expansion. Then, we can try to use them (with a corresponding increase in the level of complexity) to predict the rest of the diagram. If we need to find ε-suppressed terms, we must further increase the level of transcendentality of the corresponding basic elements.

Furthermore, using the obtained results for $F_{N,k}(n)$ and several terms (usually less than 100) that were accurately calculated, we prepare a system of algebraic equations for the parameters of the ansatz. By solving the system, we can obtain analytic results for FIs without exact calculations. In this way, the results for many complicated two-loop three-point diagrams were obtained without direct calculations (see [62,107,108,124–128]).

We would like to note that similar properties have recently been observed [73–76] in the so-called double operator–product–expansion limit of some four-point diagrams.

In N = 4 SYM, the corresponding ansatz based on the properties of maximal transcendentality turns out to be stronger than in (155): the index b in (155) should be zero. This imposes very strong restrictions on the structure of the results [47–51], including the Yang–Baxter Q-function [129,130]. These constraints allow us to obtain the anomalous dimensions [49,50] in N = 4 SYM from the QCD results [52–54] up to three loops, as well as from the Bethe ansatz [131,132] up to seven loops [133–137]. In addition, there are other results (see Refs. [138–145]) related to the principle of maximum transcendentality [47–51].

8.4. Modern Method of Massive FIs

The coefficients of the inverse-mass expansions have the properties (163) and (166) in accordance with the rule (164). Note that this rule leads to a significant decrease in the possible coefficients. This limitation is due to the DE specific form for the FIs studied in this section. These DEs can be formally represented in the following form [55–59]

$$\left((x+a)\frac{d}{dx} - \bar{k}\varepsilon \right) \mathrm{FI} \;=\; \text{simpler FIs} (\equiv \mathrm{FI}_1), \tag{167}$$

with some number a and some function $\bar{k}(x)$. We exactly show that the IT in the DE (167) contains only simpler diagrams. Note that the DE form is generated by the IBP relations for an internal n-leg single-loop subgraph, which in turn contains the product $k^{\mu_1}k^{\mu_2}k^{\mu_3}...k^{\mu_m}$ of the internal momentum k at $m = n - 3$.

Indeed, for the usual values $\alpha_i = 1 + a_i\varepsilon$ of the degrees of propagators of a subgraph with arbitrary a_i, the IBP relation (14) gives a coefficient $d - 2\alpha_1 - \sum_{i=2}^{p}\alpha_i + m\sin\varepsilon$ for the FI itself with $m = n - 3$. Important examples of applying this rule are FIs I_1, I_{12} and P_5, P_{12}, P_{126} (for the cases of $n = 2$ and $n = 3$), as well as FIs in [67] (for the cases $n = 3$ and $n = 4$). However, we note that the results for non-planar FIs (see Figure 3 in [62]) obey the property (166), but their subgraphs do not correspond to the obtained rule, which may be due to the on-shall vertex of the subgraph. However, this requires additional research.

Taking a set of simpler FIs, such as FI_1 (collected in IT of the DE (167)), we obtain their structure like in Equation (166), but with a lower level of transcendentality.

So, the FIs FI_1 must obey the following DE in the formal form

$$\left((x + a_1) \frac{d}{dx} - \bar{k}_1 \varepsilon \right) FI_1 = \text{simpler}^2 \text{ FIs} (\equiv FI_2). \tag{168}$$

Thus, we have the DE set for all FIs FI_n as

$$\left((x + a_n) \frac{d}{dx} - \bar{k}_n \varepsilon \right) FI_n = \text{simpler}^{n+1} \text{ FIs} (\equiv FI_{n+1}), \tag{169}$$

with the last FI FI_{n+1} mainly containing tadpoles.

Following [146,147], we can replace the above system of inhomogeneous DEs as a homogeneous matrix DE (for complicated diagrams, see [148]; also see [149–151]. for methods to obtain homogeneous matrix DEs)

$$\frac{d}{dx} \widehat{FI} - \varepsilon \widehat{K} \widehat{FI} = 0, \tag{170}$$

for the vector

$$\widehat{FI} = \begin{pmatrix} FI \\ FI_1/'' \\ \dots \\ FI_n/\varepsilon^n \end{pmatrix},$$

where the matrix $\widehat{K}$ contains $\bar{k}_j / (x + a_j)$ as the it elements. The form was called the "canonic basic" (see (170)) and it is very popular now (see, for example, the review [152]).

In real calculations, we replace FI_n by

$$FI_n = \widetilde{FI}_n \overline{FI}_n, \tag{171}$$

where the term $\overline{FI}_n$ obeys the homogeneous Eq

$$\left((x + a_n) \frac{d}{dx} - \bar{k}_n \varepsilon \right) \overline{FI}_n = 0, \tag{172}$$

The replacement (171) simplifies the above DE (169) as

$$(x + a_n) \frac{d}{dx} \widetilde{FI}_n = \widetilde{FI}_{n+1} \frac{\overline{FI}_{n+1}}{\overline{FI}_n}, \tag{173}$$

having the it solution as

$$\widetilde{FI}_n(x) = \int_0^x \frac{dx_1}{x_1 + a_n} \widetilde{FI}_{n+1}(x_1) \frac{\overline{FI}_{n+1}(x_1)}{\overline{FI}_n(x_1)} \tag{174}$$

There are often some abbreviations for $\overline{FI}_{n+1}/\overline{FI}_n$, so it is equal to 1. In this case, Equation (174) matches with the definition of Goncharov polylogarithms [153–155].

The results (161), (162), and (165) can be expressed in the form of Nilson [112] and Remiddi–Vermaseren [156] polylogarithms with the weigh $4 - N$ (see [62,124]). A consideration of more complicated cases can be found in Ref. [157].

9. Conclusions

In this review, we reviewed effective methods for calculating FIs, as well as examples of the application of these methods. In the massless case, we studied the scalar two-point FIs with a TP in the numerator of one of the propagators, as well as FIs depending on the

two momenta q and p when $p^2 = 0$. We also looked at FIs up to and including five loops that contribute to the β-function of the φ^4 model. The FI results were analytically obtained in [8,13]; however, they were published without intermediate calculations. Our calculations are performed in detail.

In the case of massive propagators, we calculated of one of the complicated FIs that contribute to the ratio of the $\overline{MS}$ mass to the pole mass of the Higgs boson in the standard model in the limit of the heavy Higgs boson. The results for this FI were obtained by the DE method. They contain logarithms and dilogarithms with unusual arguments.

In addition, in the massive case, we studied the inverse-mass expansion for some two-loop two- and three-point FIs . For the massive FIs under consideration, we have introduced a definition of the level of transcendentality (or complexity), or weight, which is stored for any order of ε. Moreover, it decreases in the front of logarithms or ζ-values. We called this property *transcendentality principle*. Its usage leads to the possibility of obtaining results for most FIs without direct calculations.

The transcendentality principle is violated in physical models such as QCD, where the corresponding propagators (for both quarks and gluons) have momenta in their numerators, leading to the mixing of complexity levels. However, this property is restored after diagonalization for the corresponding anomalous dimensions and coefficient functions in $N = 4$ SYM, which is an excellent, but so far little-studied property.

Conflicts of Interest: The author declares no conflict of interest.

Appendix A. Analytic Continuation

In Appendix A, we show the direct evaluation of the special case $C_2(1, n = 0)$ from the general result $C_2(1, n)$ shown in Equation (45) using the analytic continuation (from even n values) of the following sum

$$S_{-2}(n) = \sum_{m=1}^{n} \frac{(-1)^m}{m^2} . \tag{A1}$$

Indeed, considering $S_{-2}(n$ as an example, it is useful to show the main stages of the analytical continuation (see Ref. [158,159] and the references and discussions therein). For more general nested sums $S_{\pm a, \pm b, \dots}(n)$, the results are more complicated, which may make it difficult to understand the analytical continuation.

The main idea of analytical continuation is simple: remove the argument n from the sum upper limit. After performing this procedure, we have the opportunity to expand and to differentiate with respect to n.

Firstly, the sum $S_{-2}(n)$ in Equation (A1) is represented as

$$S_{-2}(n) = \left(\sum_{m=1}^{\infty} - \sum_{m=n+1}^{\infty} \right) \frac{(-1)^m}{m^2} = S_{-2}(\infty) - (-1)^n \sum_{m=1}^{\infty} \frac{(-1)^m}{(m+n)^2} . \tag{A2}$$

and the unpleasant multiplier $(-1)^n$ comes in the front of the last term in the r.h.s.

In the new sum $(-1)^n S_{-2}(n)$

$$(-1)^n S_{-2}(n) = (-1)^n S_{-2}(\infty) - \sum_{m=1}^{\infty} \frac{(-1)^m}{(m+n)^2} , \tag{A3}$$

the factor $(-1)^n$ is moved to the first term.

Now, we consider the new sum $\overline{S}_{-2}(n)$ in the form

$$\overline{S}_{-2}(n) = (-1)^n S_{-2}(n) + (1 - (-1)^n) S_{-2}(\infty), \tag{A4}$$

which is equal to the original $S_{-2}(n)$ for even n values and has no the factor $(-1)^n$:

$$\overline{S}_{-2}(n) = S_{-2}(\infty) - \sum_{m=1}^{\infty} \frac{(-1)^m}{(m+n)^2}. \tag{A5}$$

Thus, the sum $\overline{S}_{-2}(n)$ can be taken as an analytic continuation (from even n values) of the initial sum $S_{-2}(n)$.

Now, we can consider the limit $C_2(1, n)$ for small n for $\overline{S}_{-2}(n)$:

$$
\begin{aligned}
\overline{S}_{-2}(n = \delta \to 0) &= S_{-2}(\infty) - \sum_{m=1}^{\infty} \frac{(-1)^m}{m^2} \left[1 - 2\frac{\delta}{m} + O(\delta^2) \right] \\
&= 2\delta \sum_{m=1}^{\infty} \frac{(-1)^m}{m^3} + O(\delta^2) = 2\delta\, S_{-3}(\infty) + O(\delta^2).
\end{aligned} \tag{A6}
$$

In the r.h.s., the function $S_{-3}(\infty)$ is equal to the Euler number $\overline{\zeta}_3$:

$$\overline{\zeta}_a = \sum_{m=1}^{\infty} \frac{(-1)^m}{m^a} = \left(\frac{1}{2^a} - 1 \right) \zeta_a = -\frac{3}{4} \zeta_3 \text{ for } a = 3. \tag{A7}$$

So, in the small n limit, we have for $\overline{S}_{-2}(n)$:

$$\overline{S}_{-2}(n = \delta \to 0) = -\frac{3}{4} \zeta_3 \delta + O(\delta^2) \tag{A8}$$

and for the coefficient $C_2(1, n = 0)$ in Equation (45)

$$C_2(1, n = 0) = -\frac{4}{\delta(1 + \delta)} \overline{S}_{-2}(n = \delta \to 0) = 6\zeta_3 + O(\delta), \tag{A9}$$

which is exactly the same as $C_1(1, n = 0)$.

The analytical continuation is applicable in many important cases, such as, for example, studying the Q^2-evolutions of parton densities and deep-inelastic structure functions. The [160] approach is popular, based on the Jacobi polynomials, which, in turn, are related to the Mellin moments of parton distributions. Usually, only even or odd Mellin moments can be accurately calculated. Using the Q^2-evolution for the moments, defined by the simple DGLAP DEs [161–165], in the last step, parton densities and/or structure functions are recovered by summing (up to some value N_{MAX}) Jacobi polynomials.

In such an analysis, the Q^2-evolution must be carried out for both even and odd moments, so the analytic continuation is necessary. A large number of QCD analyses of experimental data were performed using it (see the review in [166]).

Another important use of the analytical continuation is the study [167] (see also the references and discussions therein) of parton densities and structure functions in the region of small values of the Bjorken variable x, which is directly related to the aforementioned studies of nested sums in the limit $n \to 0$. The approach includes the extraction of gluon distribution and the longitudinal structure function F_L from the data for the structural function F_2, the Q^2-evolution of parton densities at a small x in the nucleon and in nuclei, and the asymptotics of the cross-section at ultrahigh energies for the interaction of neutrinos with hadrons. Some overview of these studies is given in Ref. [168].

Appendix B. The Method of "Projectors"

In Refs. [20–22], we applied a special case of the "projectors" method [94–97]—the "differentiation" method, which makes it possible to calculate a FI, which depended on two momenta p and q, when $p^2 = 0$, i.e., obtain the coefficients at the $[2(pq)]/q^2$ powers. These coefficients are called "moments" of the considered FI.

As a first example, we consider the FI $J_1(\alpha, q, p)$:

$$
J_1(\alpha, q, p) = \cdots \Big|_{p^2=0} = \sum_k J(\alpha, k) \frac{2^k p_{\lambda_1} p_{\lambda_2} p_{\lambda_3} \cdots p_{\lambda_k} q^{\lambda_1} q^{\lambda_2} q^{\lambda_3} \cdots q^{\lambda_k}}{q^{2(k+\alpha+2\varepsilon)}} , \tag{A10}
$$

Now, we differentiate Equation (A10) on both sides n times with respect to p and set $p = 0$. In the l.h.s., we obtain

$$
\frac{d}{dp_{\mu_1}} \frac{d}{dp_{\mu_2}} \frac{d}{dp_{\mu_3}} \cdots \frac{d}{dp_{\mu_n}} \left\{ \cdots \right\} \Big|_{p=0} = \hat{S} \frac{2^n \Gamma(n+\alpha)}{\Gamma(\alpha)} \cdots ,
$$

where $\hat{S}$ is a symmetrization factor on indices: λ_i, μ_j ($i = 1, 2, 3, \ldots, m,\ j = 1, 2, 3, \ldots, n$).

In the r.h.s., we have

$$
\sum_k J_1(\alpha, k) \frac{2^k q^{\nu_1} q^{\nu_2} q^{\nu_3} \cdots q^{\nu_k}}{q^{2(k+\alpha+2\varepsilon)}} \frac{d}{dp_{\mu_1}} \frac{d}{dp_{\mu_2}} \frac{d}{dp_{\mu_3}} \cdots \frac{d}{dp_{\mu_n}} \left(p^{\nu_1} p^{\nu_2} p^{\nu_3} \cdots p^{\nu_k} \right) \Big|_{p=0} = \hat{S}\, n!\, J_1(\alpha, n) \frac{2^n q^{\nu_1} q^{\nu_2} q^{\nu_3} \cdots q^{\nu_n}}{q^{2(n+\alpha+2\varepsilon)}} .
$$

So, for the moments $J_1(\alpha, n)$, we have the following expression:

$$
J_1(\alpha, n) \frac{q^{\nu_1} q^{\nu_2} q^{\nu_3} \cdots q^{\nu_n}}{q^{2(n+\alpha+2\varepsilon)}} = \hat{S} \frac{\Gamma(n+\alpha)}{n!\,\Gamma(\alpha)} \cdots \overset{\alpha=1}{=} \hat{S} \cdots .
$$

In what follows, we neglect the symmetrizer $\hat{S}$.

We would like to draw attention to the fact that this transformation from the FI at its moment remains correct for arbitrary indices of the FI lines, as well as in the presence of additional momenta in the FI propagators (if the latter are located on a differentiable line, then small changes will be required).

As a second example, we consider

$$
\bar{J}_1(\alpha, q, p) = \cdots
$$

By full analogy with the previous FI, for its moments, we obtain:

$$\bar{J}_1(\alpha, n) \frac{q^{\nu_1} q^{\nu_2} q^{\nu_3} \dots q^{\nu_n}}{q^{2(n+\alpha+2\varepsilon)}} = \hat{S} \frac{\Gamma(n+\alpha)}{n!\Gamma(\alpha)} \quad \overset{\alpha=1}{=} \hat{S}$$

Rather similar conclusions can be also drawn for the FI

$$\hat{J}_1(\alpha, \beta, q, p) =$$

Its moment has the form

$$\hat{J}_1(\alpha, \beta, n) \frac{q^{\nu_1} q^{\nu_2} q^{\nu_3} \dots q^{\nu_n}}{q^{2(n+\alpha+2\varepsilon)}} = \sum_{k=0}^{n} \frac{\Gamma(k+\beta)\Gamma(n-k+\alpha)}{(n-k)!k!\Gamma(\alpha)\Gamma(\beta)}$$

$$\overset{\alpha=\beta=1}{=} \sum_{k=0}^{n}$$

We would like to note that there is another method for calculating the FIs in question: the method of "gluing" [169]. Using the TP orthogonality, it is possible to obtain the moment of the FI in question by further integrating the original FI along the momentum q with a propagator that has some special index δ and the additional TP in its numerator. This additional integration produces very complex three-loop FIs. So, for the FIs under consideration $J_1(\alpha, q, p)$, $\bar{J}_1(\alpha, q, p)$, $\hat{J}_1(\alpha, \beta, q, p)$, these "glued" three-loop FIs have the following view
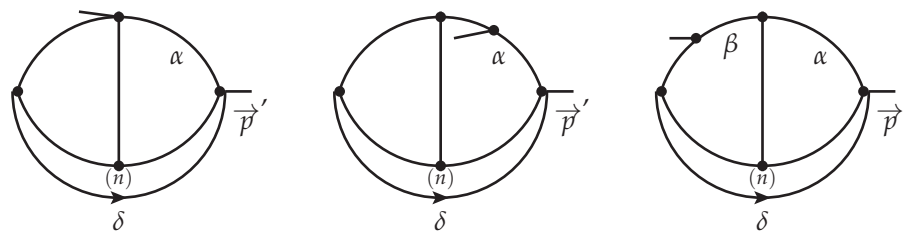
The calculation of these complex FIs is above the slope of the paper. Some examples of the usage of the "gluing" method can be found in Ref. [15].

As a conclusion of Appendix B, we would like to note that, when using the method of 'projectors' [94–97], expressions obtained for the *n*th moment of the original FI always look much simpler than when using the "gluing" method [169].

Appendix C. Useful Variables for Integrations

Here, we give sets of new integration variables that are useful in the case of on-shall massive FIs.

$$t^2 = \frac{z}{4-z}, \quad z = \frac{4t^2}{1+t^2}, \quad 4-z = \frac{4}{1+t^2}, \quad (dz) = \frac{8t(dt)}{(1+t^2)^2};$$

$$y = \frac{1-it}{1+it}, \quad t = \frac{1-y}{i(1+y)}, \quad 1+t^2 = \frac{4y}{(1+y)^2}, \quad (dt) = -\frac{2}{i}\frac{(dy)}{(1+y)^2}, \quad \frac{(dt)}{1+t^2} = -\frac{1}{2i}\frac{(dy)}{y};$$

$$\xi = \frac{1-\sqrt{3}t}{1+\sqrt{3}t}, \quad t = \frac{1}{\sqrt{3}}\frac{1-\xi}{1+\xi}, \quad z = \frac{4t^2}{1+t^2} = \frac{(1-\xi)^2}{1+\xi+\xi^2} = \frac{(1-\xi)^3}{1-\xi^3},$$

$$(dt) = -\frac{2(dy)}{\sqrt{3}(1+y)^2}, \quad \frac{(dt)}{1-3t^2} = -\frac{1}{2\sqrt{3}}\frac{(d\xi)}{\xi}. \tag{A11}$$

References

1. Peterman, A. Renormalization Group and the Deep Structure of the Proton. *Phys. Rep.* **1979**, *53*, 157–248. [CrossRef]
2. 't Hooft, G.; Veltman, M.J.G. Regularization and Renormalization of Gauge Fields. *Nucl. Phys. B* **1972**, *44*, 189–213. [CrossRef]
3. Bollini, C.G.; Giambiagi, J.J. Dimensional Renormalization: The Number of Dimensions as a Regularizing Parameter. *Nuovo Cim. B* **1972**, *12*, 20–26. [CrossRef]
4. Cicuta, G.M.; Montaldi, E. Analytic renormalization via continuous space dimension. *Lett. Nuovo Cim.* **1972**, *4*, 329–332. [CrossRef]
5. Hooft, G. Dimensional regularization and the renormalization group. *Nucl. Phys. B* **1973**, *61*, 455–468. [CrossRef]
6. D'Eramo, M.; Peliti, L. Theoretical Predictions for Critical Exponents at the Lambda Point of Bose Liquids. *Lett. Nuovo Cim.* **1971**, *2*, 878–880. [CrossRef]
7. Vasiliev, A.N.; Khonkonen, Y.R. 1/N Expansion: Calculation of the Exponents Eta Furthermore, Nu in the Order 1/N**2 for Arbitrary Number of Dimensions. *Theor. Math. Phys.* **1981**, *47*, 465–475. [CrossRef]
8. Kazakov, D.I. The Method of Uniqueness, a New Powerful Technique for Multiloop Calculations. *Phys. Lett. B* **1983**, *133*, 406–410. [CrossRef]
9. Kazakov, D.I. Calculation of Feynman Integrals by the Method of 'uniqueness'. *Theor. Math. Phys.* **1984**, *58*, 223–230. [*Teor. Mat. Fiz.* **1984**, *58*, 343]. [CrossRef]
10. Usyukina, N.I. Calculation of Many Loop Diagrams of Perturbation Theory. *Theor. Math. Phys.* **1983**, *54*, 78–81. [*Teor. Mat. Fiz.* **1983**, *54*, 124]. [CrossRef]
11. Belokurov, V.V.; Usyukina, N.I.J. Calculation of Ladder Diagrams in Arbitrary Order. *J. Phys. A* **1983**, *16*, 2811. [CrossRef]
12. Belokurov, V.V.; Usyukina, N.I. An Algorithm for Calculating Massless Feynman Diagrams. *Theor. Math. Phys.* **1989**, *79*, 385–391. [*Teor. Mat. Fiz.* **1989**, *79*, 63].
13. Kazakov, D.I. Multiloop Calculations: Method of Uniqueness and Functional Equations. *Theor. Math. Phys.* **1985**, *62*, 84–89. [*Teor. Mat. Fiz.* **1984**, *62*, 127]. [CrossRef]
14. Kotikov, A.V. The Gegenbauer polynomial technique: The Evaluation of a class of Feynman diagrams. *Phys. Lett. B* **1996**, *375*, 240–248. [CrossRef]
15. Kotikov, A.V.; Teber, S. New Results for a Two-Loop Massless Propagator-Type Feynman Diagram. *Theor. Math. Phys.* **2018**, *194*, 284–294. [*Teor. Mat. Fiz.* **2018**, *194*, 331]. [CrossRef]
16. Kotikov, A.V.; Teber, S. Multi-loop techniques for massless Feynman diagram calculations. *Phys. Part. Nucl.* **2019**, *50*, 1–41. [CrossRef]
17. Kotikov, A.V. Differential Equations and Feynman Integrals. *arXiv* **2012**, arXiv:2102.07424.
18. Ryder, L.H. *Quantum Field Theory*; Cambridge University Press: Cambridge, UK, 1996.
19. Chetyrkin, K.G.; Tkachov, F.V. Integration By Parts: The Algorithm to Calculate Beta Functions in 4 Loops. *Nucl. Phys. B* **1981**, *192*, 159–204. [CrossRef]
20. Kazakov, D.I.; Kotikov, A.V. The Method of Uniqueness: Multiloop Calculations in QCD. *Theor. Math. Phys.* **1988**, *73*, 1264–1274. [CrossRef]
21. Kazakov, D.I.; Kotikov, A.B. Total α_s Correction to Deep Inelastic Scattering Cross-section Ratio R = σ_L/σ_T in QCD. *Nucl. Phys. B* **1988**, *307*, 721–762; Erratum in *Nucl. Phys. B* **1990**, *345*, 299. [CrossRef]
22. Kotikov, A.V. The Calculation of Moments of Structure Function of Deep Inelastic Scattering in QCD. *Theor. Math. Phys.* **1989**, *78*, 134–143. [CrossRef]
23. Kotikov, A.V. Differential equations method: New technique for massive Feynman diagrams calculation. *Phys. Lett. B* **1991**, *254*, 158–164. [CrossRef]
24. Kotikov, A.V. Differential equations method: The Calculation of vertex type Feynman diagrams. *Phys. Lett. B* **1991**, *259*, 314–322. [CrossRef]
25. Kotikov, A.V. Differential equation method: The Calculation of N point Feynman diagrams. *Phys. Lett. B* **1991**, *267*, 123–127. [CrossRef]
26. Kotikov, A.V. New method of massive N point Feynman diagrams calculation. *Mod. Phys. Lett. A* **1991**, *6*, 3133–3141. [CrossRef]

27. Remiddi, E. Differential equations for Feynman graph amplitudes. *Nuovo Cim. A* **1997**, *110*, 1435–1452. [CrossRef]
28. Kotikov, A.V. New method of massive Feynman diagrams calculation. *Mod. Phys. Lett. A* **1991**, *6*, 677–692. [CrossRef]
29. Kotikov, A.V. New method of massive Feynman diagrams calculation. Vertex type functions. *Int. J. Mod. Phys. A* **1992**, *7*, 1977–1991. [CrossRef]
30. Gorishnii, S.G.; Larin, S.A.; Tkachov, F.V.; Chetyrkin, K.G. Five Loop Renormalization Group Calculations in the $g\phi^4$ in Four-dimensions Theory. *Phys. Lett. B* **1983**, *132*, 351–354.
31. Tarasov, O.V. Connection between Feynman integrals having different values of the space-time dimension. *Phys. Rev. D* **1996**, *54*, 6479. [CrossRef]
32. Tarasov, O.V. Generalized recurrence relations for two loop propagator integrals with arbitrary masses. *Nucl. Phys. B* **1997**, *502*, 455–482. [CrossRef]
33. Lee, R.N. Presenting LiteRed: A tool for the Loop InTEgrals REDuction. *arXiv* **2012**, arXiv:1212.2685.
34. Lee, R.N. LiteRed 1.4: A powerful tool for reduction of multiloop integrals. *J. Phys. Conf. Ser.* **2014**, *523*, 012059. [CrossRef]
35. Lee, R.N.; Smirnov, A.V.; Smirnov, V.A. Analytic Results for Massless Three-Loop Form Factors. *J. High Energy Phys. JHEP* **2010**, *1004*, 020. [CrossRef]
36. Kotikov, A.V.; Lipatov, L.N. NLO corrections to the BFKL equation in QCD and in supersymmetric gauge theories. *Nucl. Phys. B* **2000**, *582*, 19–43. [CrossRef]
37. Lipatov, L.N. Reggeization of the Vector Meson and the Vacuum Singularity in Nonabelian Gauge Theories. *Sov. J. Nucl. Phys.* **1976**, *23*, 338–345.
38. Fadin, V.S.; Kuraev, E.A.; Lipatov, L.N. On the Pomeranchuk Singularity in Asymptotically Free Theories. *Phys. Lett. B* **1975**, *60*, 50–52. [CrossRef]
39. Kuraev, E.A.; Lipatov, L.N.; Fadin, V.S. Multi-Reggeon Processes in the Yang-Mills Theory. *Sov. Phys. JETP* **1976**, *44*, 443–450.
40. Kuraev, E.A.; Lipatov, L.N.; Fadin, V.S. The Pomeranchuk Singularity in Nonabelian Gauge Theories. *Sov. Phys. JETP* **1977**, *45*, 199–204.
41. Balitsky, I.I.; Lipatov, L.N. The Pomeranchuk Singularity in Quantum Chromodynamics. *Sov. J. Nucl. Phys.* **1978**, *28*, 822–829.
42. Balitsky, I.I.; Lipatov, L.N. Calculation of meson meson interaction cross-section in quantum chromodynamics. *JETP Lett.* **1979**, *30*, 355.
43. Fadin, V.S.; Lipatov, L.N. BFKL pomeron in the next-to-leading approximation. *Phys. Lett. B* **1998**, *429*, 127–134. [CrossRef]
44. Camici, G.; Ciafaloni, M. Energy scale(s) and next-to-leading BFKL equation. *Phys. Lett. B* **1998**, *430*, 349–354.
45. Brink, L.; Schwarz, J.H.; Scherk, J. Supersymmetric Yang-Mills Theories. *Nucl. Phys. B* **1977**, *121*, 77–92. [CrossRef]
46. Gliozzi, F.; Scherk, J.; Olive, D.I. Supersymmetry, Supergravity Theories and the Dual Spinor Model. *Nucl. Phys. B* **1977**, *122*, 253–290. [CrossRef]
47. Kotikov, A.V.; Lipatov, L.N. DGLAP and BFKL equations in the N = 4 supersymmetric gauge theory. *Nucl. Phys. B* **2003**, *661*, 19–61. [CrossRef]
48. Kotikov, A.V.; Lipatov, L.N. DGLAP and BFKL evolution equations in the N = 4 supersymmetric gauge theory. *arXiv* **2001**, arXiv:hep-ph/0112346.
49. Kotikov, A.V.; Lipatov, L.N.; Velizhanin, V.N. Anomalous dimensions of Wilson operators in N = 4 SYM theory. *Phys. Lett. B* **2003**, *557*, 114–120. [CrossRef]
50. Kotikov, A.V.; Lipatov, L.N.; Onishchenko, A.I.; Velizhanin, V.N. Three loop universal anomalous dimension of the Wilson operators in N = 4 SUSY Yang-Mills model. *Phys. Lett. B* **2004**, *595*, 521–529. [CrossRef]
51. Bianchi, L.; Forini, V.; Kotikov, A.V. On DIS Wilson coefficients in N=4 super Yang–Mills theory. *Phys. Lett. B* **2013**, *725*, 394–401. [CrossRef]
52. Moch, S.; Vermaseren, J.A.M.; Vogt, A. The Three loop splitting functions in QCD: The Nonsinglet case. *Nucl. Phys. B* **2004**, *688*, 101–134. [CrossRef]
53. Vogt, A.; Moch, S.; Vermaseren, J.A.M. The Three-loop splitting functions in QCD: The Singlet case. *Nucl. Phys. B* **2004**, *691*, 129–181. [CrossRef]
54. Vermaseren, J.A.M.; Vogt, A.; Moch, S. The Third-order QCD corrections to deep-inelastic scattering by photon exchange. *Nucl. Phys. B* **2005**, *724*, 3–182. [CrossRef]
55. Kotikov, A.V. The Property of maximal transcendentality in the N = 4 Supersymmetric Yang–Mills. In *Subtleties in Quantum Field Theory*; Diakonov, D., Ed.; PNPI: Gatchina, Russia, 2010; pp. 150–174.
56. Kotikov, A.V. The property of maximal transcendentality: Calculation of anomalous dimensions in the $\mathcal{N}$ = 4 SYM and master integrals. *Phys. Part. Nucl.* **2013**, *44*, 374–385. [CrossRef]
57. Kotikov, A.V.; Onishchenko, A.I. DGLAP and BFKL equations in $\mathcal{N}$ = 4 SYM: From weak to strong coupling. *arXiv* **2019**, arXiv:1908.05113.
58. Kotikov, A.V. The property of maximal transcendentality: Calculation of master integrals. *Theor. Math. Phys.* **2013**, *176*, 913–921. [CrossRef]
59. Kotikov, A.V. The property of maximal transcendentality: Calculation of Feynman integrals. *Theor. Math. Phys.* **2017**, *190*, 391–401. [CrossRef]
60. Kotikov, A.V. Some Examples of Calculation of Massless and Massive Feynman Integrals. *Particles* **2021**, *4*, 361–380. [CrossRef]
61. Broadhurst, D.J. The Master Two Loop Diagram with Masses. *Z. Phys. C* **1990**, *47*, 115–124. [CrossRef]

62. Fleischer, J.; Kotikov, A.V.; Veretin, O.L. Analytic two loop results for selfenergy type and vertex type diagrams with one nonzero mass. *Nucl. Phys. B* **1999**, *547*, 343–374. [CrossRef]
63. Kotikov, A.V. About calculation of massless and massive Feynman integrals. *Particles* **2020**, *3*, 394–443. [CrossRef]
64. Eden, B.; Heslop, P.; Korchemsky, G.P.; Sokatchev, E. Hidden symmetry of four-point correlation functions and amplitudes in N = 4 SYM. *Nucl. Phys. B* **2012**, *862*, 193–231. [CrossRef]
65. Dixon, L.J. Scattering amplitudes: The most perfect microscopic structures in the universe. *J. Phys. A* **2011**, *44*, 454001. [CrossRef]
66. Dixon, L.J.; Drummond, J.M.; Henn, J.M. Analytic result for the two-loop six-point NMHV amplitude in N = 4 super Yang–Mills theory. *J. High Energy Phys. JHEP* **2012**, *2012*, 024. [CrossRef]
67. Gehrmann, T.; Henn, J.M.; Huber, T. The three-loop form factor in N = 4 super Yang–Mills. *J. High Energy Phys. JHEP* **2012**, *2012*, 101. [CrossRef]
68. Brandhuber, A.; Travaglini, G.; Yang, G. Analytic two-loop form factors in N = 4 SYM. *J. High Energy Phys. JHEP* **2012**, *2012*, 082. [CrossRef]
69. Henn, J.M.; Moch, S.; Naculich, S.G. Form factors and scattering amplitudes in N = 4 SYM in dimensional and massive regularizations. *J. High Energy Phys. JHEP* **2011**, *2011*, 024. [CrossRef]
70. Schlotterer, O.; Stieberger, S.J. Motivic Multiple Zeta Values and Superstring Amplitudes. *J. Phys. A* **2013**, *46*, 475401. [CrossRef]
71. Broedel, J.; Schlotterer, O.; Stieberger, S. Polylogarithms, Multiple Zeta Values and Superstring Amplitudes. *Fortsch. Phys.* **2013**, *61*, 812–870. [CrossRef]
72. Stieberger, S.; Taylor, T.R. Maximally Helicity Violating Disk Amplitudes, Twistors and Transcendental Integrals. *Phys. Lett. B* **2012**, *716*, 236–239. [CrossRef]
73. Eden, B. Three-loop universal structure constants in N=4 susy Yang–Mills theory. *arXiv* **2012**, arXiv:1207.3112.
74. Ambrosio, R.G.; Eden, B.; Goddard, T.; Heslop, P.; Taylor, C. Local integrands for the five-point amplitude in planar N=4 SYM up to five loops. *J. High Energy Phys. JHEP* **2015**, *2015*, 116. [CrossRef]
75. Chicherin, D.; Doobary, R.; Eden, B.; Heslop, P.; Korchemsky, G.P.; Sokatchev, E. Bootstrapping correlation functions in N = 4 SYM. *J. High Energy Phys. JHEP* **2016**, *2016*, 031. [CrossRef]
76. Eden, B.; Sfondrini, A. Three-point functions in $\mathcal{N} = 4$ SYM: The hexagon proposal at three loops. *J. High Energy Phys. JHEP* **2016**, *2016*, 165. [CrossRef]
77. Chetyrkin, K.G.; Kataev, A.L.; Tkachov, F.V. New Approach to Evaluation of Multiloop Feynman Integrals: The Gegenbauer Polynomial x Space Technique. *Nucl. Phys. B* **1980**, *174*, 345–377. [CrossRef]
78. Kotikov, A.V. Critical behavior of 3-D electrodynamics. *JETP Lett.* **1993**, *58*, 731. [*Pisma Zh. Eksp. Teor. Fiz.* **1993**, *58*, 785].
79. Kotikov, A.V. On the Critical Behavior of (2+1)-Dimensional QED. *Phys. Atom. Nucl.* **2012**, *75*, 890–892. [CrossRef]
80. Kotikov, A.V.; Shilin, V.I.; Teber, S. Critical behavior of (2+1)-dimensional QED: $1/N_f$ corrections in the Landau gauge. *Phys. Rev. D* **2016**, *94*, 056009; Erratum in *Phys. Rev. D* **2019**, *99*, 119901. [CrossRef]
81. Kotikov, A.V.; Teber, S. Critical behavior of (2+1)-dimensional QED: $1/N_f$ corrections in an arbitrary nonlocal gauge. *Phys. Rev. D* **2016**, *94*, 114011; Addendum in *Phys. Rev. D* **2019**, *99*, 059902. [CrossRef]
82. Kotikov, A.V.; Teber, S. Two-loop fermion self-energy in reduced quantum electrodynamics and application to the ultrarelativistic limit of graphene. *Phys. Rev. D* **2014**, *89*, 065038. [CrossRef]
83. Derkachev, S.E.; Ivanov, A.V.; Shumilov, L.A. Mellin–Barnes transformation for two-loop master-diagrams. *Zap. Nauchn. Semin.* **2020**, *494*, 144–167. [CrossRef]
84. Derkachev, S.E.; Ivanov, A.V.; Shumilov, L.A. Mellin–Barnes Transformation for Two-Loop Master-Diagram. *J. Math. Sci.* **2022**, *264*, 298–312. [CrossRef]
85. Derkachev, S.E.; Isaev, A.P.; Shumilov, L.A. Ladder and zig-zag Feynman diagrams, operator formalism and conformal triangles. *J. High Energy Phys. JHEP* **2023**, *2023*, 059. [CrossRef]
86. Teber, S.; Kotikov, A.V. The method of uniqueness and the optical conductivity of graphene: New application of a powerful technique for multiloop calculations. *Theor. Math. Phys.* **2017**, *190*, 446–457. [CrossRef]
87. Tkachov, F.V. A Theorem on Analytical Calculability of Four Loop Renormalization Group Functions. *Phys. Lett. B* **1981**, *100*, 65–68. [CrossRef]
88. Broadhurst, D.J. Exploiting the 1.440 Fold Symmetry of the Master Two Loop Diagram. *Z. Phys. C* **1986**, *32*, 249-253. [CrossRef]
89. Gorishnii, S.G.; Isaev, A.P. On an Approach to the Calculation of Multiloop Massless Feynman Integrals. *Theor. Math. Phys.* **1985**, *62*, 232–240. [*Teor. Mat. Fiz.* **1985**, *62*, 345]. [CrossRef]
90. Kazakov, D.I. Analytical Methods for Multiloop Calculations: Two Lectures on The Method of Uniqueness. JINR-E2-84-410. 1984. Available online: https://inspirehep.net/literature/203305 (accessed on 25 May 2023).
91. Broadhurst, D.J. Dimensionally continued multiloop gauge theory. *arXiv* **1999**, arXiv:hep-th/9909185.
92. Kotikov, A.V.; Teber, S. Landau-Khalatnikov-Fradkin transformation and the mystery of even ζ-values in Euclidean massless correlators. *Phys. Rev. D* **2019**, *100*, 105017. [CrossRef]
93. Kazakov, D.I.; Kotikov, A.V. On the value of the alpha-s correction to the Callan-Gross relation. *Phys. Lett. B* **1992**, *291*, 171–176. [CrossRef]
94. Gorishnii, S.G.; Larin, S.A.; Tkachov, F.V. The Algorithm for Ope Coefficient Functions in the Ms Scheme. *Phys. Lett. B* **1983**, *124*, 217–220. [CrossRef]

95. Gorishnii, S.G.; Larin, S.A. Coefficient Functions of Asymptotic Operator Expansions in Minimal Subtraction Scheme. *Nucl. Phys. B* **1987**, *283*, 452–476. [CrossRef]

96. Tkachov, F.V. On The Operator Product Expansion in the Ms Scheme. *Phys. Lett. B* **1983**, *124*, 212–216. [CrossRef]

97. Chetyrkin, K.G. Infrared R*—operation and operator product expansion in the minimal subtraction scheme. *Phys. Lett. B* **1983**, *126*, 371–375. [CrossRef]

98. Bogoliubov, N.N.; Parasiuk, O.S. On the Multiplication of the causal function in thequantum theory of fields. *Acta Math.* **1957**, *97*, 227–266.

99. Hepp, K. Proof of the Bogolyubov-Parasiuk theorem on renormalization. *Commun. Math. Phys.* **1966**, *2*, 301–326. [CrossRef]

100. Zimmermann, W. Convergence of Bogoliubov's method of renormalization in momentumspace. *Commun. Math. Phys.* **1969**, *15*, 208–234. [CrossRef]

101. Vladimirov, A.A. Method for Computing Renormalization Group Functions in Dimen-sional Renormalization Scheme. *Theor. Math. Phys.* **1980**, *43*, 417–422. [CrossRef]

102. Chetyrkin, K.G.; Tkachov, F.V. Infrared R Operation Furthermore, Ultraviolet CountertermsIn The Ms Scheme. *Phys. Lett. B* **1982**, *114*, 340–344. [CrossRef]

103. Chetyrkin, K.G.; Smirnov, V.A. R* Operation Corrected. *Phys. Lett. B* **1984**, *144*, 419–424. [CrossRef]

104. Smirnov, V.A.; Chetyrkin, K.G. R* Operation in the Minimal Subtraction Scheme. *Theor. Math. Phys.* **1985**, *63*, 462–469. [CrossRef]

105. Chetyrkin, K.G. Combinatorics of R-, R^{-1}-, and R*-operations and asymptotic expan-sions of feynman integrals in the limit of large momenta and masses. *arXiv* **2017**, arXiv:1701.08627.

106. Henn, J.M.; Plefka, J.C. *Scattering Amplitudes in Gauge Theories*; Lecture Notes in Physics; Springer: Berlin, Germany, 2014; Volume 883.

107. Kniehl, B.A.; Kotikov, A.V.; Onishchenko, A.; Veretin, O. Two-loop sunset diagrams with three massive lines. *Nucl. Phys. B* **2006**, *738*, 306–316. [CrossRef]

108. Kniehl, B.A.; Kotikov, A.V.; Onishchenko, A.I.; Veretin, O.L. Two-loop diagrams in non-relativistic QCD with elliptics. *Nucl. Phys. B* **2019**, *948*, 114780. [CrossRef]

109. Kniehl, B.A.; Kotikov, A.V. Calculating four-loop tadpoles with one non-zero mass. *Phys. Lett. B* **2006**, *638*, 531–537. [CrossRef]

110. Kniehl, B.A.; Kotikov, A.V. Counting master integrals: Integration-by-parts procedure with effective mass. *Phys. Lett. B* **2012**, *712*, 233–234. [CrossRef]

111. Lewin, L. *Polylogarithms and Associated Functions*; North Holland: Amsterdam, The Netherlands, 1981.

112. Devoto, A.; Duke, D.W. Table of Integrals and Formulae for Feynman Diagram Calculations. *Riv. Nuovo Cim.* **1984**, *7*, 1–39. [CrossRef]

113. Campert, L.G.J.; Moriello, F.; Kotikov, A. Sunrise integrals with two internal masses and pseudo-threshold kinematics in terms of elliptic polylogarithms. *J. High Energy Phys. JHEP* **2021**, *2021*, 072. [CrossRef]

114. Kotikov, A.; Kuhn, J.H.; Veretin, O. Two-Loop Formfactors in Theories with Mass Gap and Z-Boson Production. *Nucl. Phys. B* **2008**, *788*, 47–62. [CrossRef]

115. Aglietti, U.; Bonciani, R. Master integrals with one massive propagator for the two loop electroweak form-factor. *Nucl. Phys. B* **2003**, *668*, 3–76. [CrossRef]

116. Aglietti, U.; Bonciani, R.; Degrassi, G.; Vicini, A. Two loop light fermion contribution to Higgs production and decays. *Phys. Lett. B* **2004**, *595*, 432–441. [CrossRef]

117. Aglietti, U.; Bonciani, R.; Degrassi, G.; Vicini, A. Master integrals for the two-loop light fermion contributions to gg —> H and H —> gamma gamma. *Phys. Lett. B* **2004**, *600*, 57–64. [CrossRef]

118. Aglietti, U.; Bonciani, R.; Degrassi, G.; Vicini, A. Analytic Results for Virtual QCD Corrections to Higgs Production and Decay. *J. High Energy Phys. JHEP* **2007**, *2007*, 021. [CrossRef]

119. Lee, R.N.; Schwartz, M.D.; Zhang, X. Compton Scattering Total Cross Section at Next-to-Leading Order. *Phys. Rev. Lett.* **2021**, *126*, 211801. [CrossRef] [PubMed]

120. Blumlein, J.; Schneider, C. Analytic Computing Methods for Precision Calculations in Quantum Field Theory. *Int. J. Mod. Phys.* **2018**, *A33*, 1830015. [CrossRef]

121. Ablinger, J.; Blümlein, J.; Schneider, C. Iterated integrals over letters induced by quadratic forms. *Phys. Rev. D* **2021**, *103*, 096025. [CrossRef]

122. Ablinger, J.; Blumlein, J.; Schneider, C.J. Harmonic Sums and Polylogarithms Generated by Cyclotomic Polynomials. *Math. Phys.* **2011**, *52*, 102301. [CrossRef]

123. Fleischer, J.; Kalmykov, M.Y.; Kotikov, A.V. Two-loop self-energy master integrals on shell. *Phys. Lett. B* **1999**, *462*, 169–177. [CrossRef]

124. Fleischer, J.; Kotikov, A.V.; Veretin, O.L. The differential equation method: Calculation of vertex-type diagrams with one non-zero mass. *Phys. Lett. B* **1998**, *417*, 163–172. [CrossRef]

125. Kniehl, B.A.; Kotikov, A.V.; Onishchenko, A.I.; Veretin, O.L. Strong-coupling constant with flavor thresholds at five loops in the MS-bar scheme. *Phys. Rev. Lett.* **2006**, *97*, 042001. [CrossRef]

126. Kniehl, B.A.; Kotikov, A.V.; Merebashvili, Z.V.; Veretin, O.L. Heavy-quark pair production in polarized photon-photon collisions at next-to-leading order: Fully integrated total cross sections. *Phys. Rev. D* **2009**, *79*, 114032. [CrossRef]

127. Kniehl, B.A.; Kotikov, A.V.; Veretin, O.L. Orthopositronium lifetime: Analytic results in $O(\alpha)$ and $O(\alpha^3 \ln(\alpha))$. *Phys. Rev. Lett.* **2008**, *101*, 193401. [CrossRef]
128. Kniehl, B.A.; Kotikov, A.V.; Veretin, O.L. Orthopositronium lifetime at O(alpha) and O(alpha^3 ln(alpha)) in closed form. *Phys. Rev. A* **2009**, *80*, 052501. [CrossRef]
129. Kotikov, A.V.; Rej, A.; Zieme, S. Analytic three-loop Solutions for N = 4 SYM Twist Operators. *Nucl. Phys. B* **2009**, *813*, 460–483. [CrossRef]
130. Beccaria, M.; Belitsky, A.V.; Kotikov, A.V.; Zieme, S. Analytic solution of the multiloop Baxter equation. *Nucl. Phys. B* **2010**, *827*, 565–606. [CrossRef]
131. Staudacher, M. The Factorized S-matrix of CFT/AdS. *J. High Energy Phys. JHEP* **2005**, *2005*, 054. [CrossRef]
132. Beisert, N.; Staudacher, M. Long-range psu(2,2|4) Bethe Ansatze for gauge theory and strings. *Nucl. Phys. B* **2005**, *727*, 1–62. [CrossRef]
133. Kotikov, A.V.; Lipatov, L.N.; Rej, A.; Staudacher, M.; Velizhanin, V.N. Dressing and wrapping. *J. Stat. Mech.* **2007**, *0710*, P10003. [CrossRef]
134. Bajnok, Z.; Janik, R.A.; Lukowski, T. our-loop perturbative Konishi from strings and finite size effects for multiparticle states. *Nucl. Phys. B* **2009**, *816*, 376–398. [CrossRef]
135. Lukowski, T.; Rej, A.; Velizhanin, V.N. Five-Loop Anomalous Dimension of Twist-Two Operators. *Nucl. Phys. B* **2010**, *831*, 105–132. [CrossRef]
136. Marboe, C.; Velizhanin, V.; Volin, D. Six-loop anomalous dimension of twist-two operators in planar $\mathcal{N} = 4$ SYM theory. *J. High Energy Phys. JHEP* **2015**, *2015*, 084. [CrossRef]
137. Marboe, C.; Velizhanin, V. Twist-2 at seven loops in planar $\mathcal{N} = 4$ SYM theory: Full result and analytic properties. *J. High Energy Phys. JHEP* **2016**, *2016*, 013. [CrossRef]
138. Kotikov, A.V.; Lipatov, L.N. On the highest transcendentality in N = 4 SUSY. *Nucl. Phys. B* **2007**, *769*, 217–255. [CrossRef]
139. Benna, M.K.; Benvenuti, S.; Klebanov, I.R.; Scardicchio, A. A Test of the AdS/CFT correspondence using high-spin operators. *Phys. Rev. Lett.* **2007**, *98*, 131603. [CrossRef] [PubMed]
140. Basso, B.; Korchemsky, G.P.; Kotanski, J. Cusp anomalous dimension in maximally supersymmetric Yang–Mills theory at strong coupling. *Phys. Rev. Lett.* **2008**, *100*, 091601. [CrossRef] [PubMed]
141. Basso, B.; Korchemsky, G.P. Embedding nonlinear O(6) sigma model into N=4 super-Yang–Mills theory. *Nucl. Phys. B* **2009**, *807*, 397–423. [CrossRef]
142. Costa, M.S.; Goncalves, V.; Penedones, J. Conformal Regge theory. *J. High Energy Phys. JHEP* **2012**, *2012*, 091. [CrossRef]
143. Kotikov, A.V.; Lipatov, L.N. Pomeron in the N=4 supersymmetric gauge model at strong couplings. *Nucl. Phys. B* **2013**, *874*, 889–904. [CrossRef]
144. Gromov, N.; Levkovich-Maslyuk, F.; Sizov, G.; Valatka, S. Quantum spectral curve at work: From small spin to strong coupling in $\mathcal{N} = 4$ SYM. *J. High Energy Phys. JHEP* **2014**, *2014*, 156. [CrossRef]
145. Alday, L.F.; Hansen, T. The AdS Virasoro-Shapiro Amplitude. *arXiv* **2023**, arXiv:2306.12786.
146. Henn, J.M. Multiloop integrals in dimensional regularization made simple. *Phys. Rev. Lett.* **2013**, *110*, 251601. [CrossRef]
147. Henn, J.M. Lectures on differential equations for Feynman integrals. *J. Phys. A* **2015**, *48*, 153001. [CrossRef]
148. Adams, L.; Weinzierl, S. The ε-form of the differential equations for Feynman integrals in the elliptic case. *Phys. Lett. B* **2018**, *781*, 270–278. [CrossRef]
149. Lee, R.N. Reducing differential equations for multiloop master integrals. *J. High Energy Phys. JHEP* **2015**, *2015*, 108. [CrossRef]
150. Lee, R.N. Symmetric ϵ- and (ϵ+1/2)-forms and quadratic constraints in "elliptic" sectors. *J. High Energy Phys. JHEP* **2018**, *2018*, 176. [CrossRef]
151. Lee, R.N.; Onishchenko, A.I. ϵ-regular basis for non-polylogarithmic multiloop integrals and total cross section of the process $e^+ e^- \to 2(Q\bar{Q})$. *J. High Energy Phys. JHEP* **2019**, *2019*, 084. [CrossRef]
152. Badger, S.; Henn, J.; Plefka, J.; Zoia, S. Scattering Amplitudes in Quantum Field Theory. *arXiv* **2023**, arXiv:2306.05976.
153. Duhr, C. Mathematical aspects of scattering amplitudes. *arXiv* **2014**, arXiv:1411.7538.
154. Goncharov, A.B. Multiple polylogarithms and mixed Tate motives. *arXiv* **2001**, arXiv:math/0103059.
155. Goncharov, A.B. Multiple polylogarithms, cyclotomy and modular complexes. *Math. Res. Lett.* **1998**, *5*, 497–516. [CrossRef]
156. Remiddi, E.; Vermaseren, J.A.M. Harmonic polylogarithms. *Int. J. Mod. Phys. A* **2000**, *15*, 725–754. [CrossRef]
157. Davydychev, A.I.; Kalmykov, M.Y. Massive Feynman diagrams and inverse binomial sums. *Nucl. Phys. B* **2004**, *699*, 3–64. [CrossRef]
158. Kotikov, A.V. Gluon distribution for small x. *Phys. At. Nucl.* **1994**, *57*, 133.
159. Kotikov, A.V.; Velizhanin, V.N. Analytic continuation of the Mellin moments of deep inelastic structure functions. *arXiv* **2005**, arXiv:hep-ph/0501274.
160. Parisi, G.; Sourlas, N. A Simple Parametrization of the Q^2 Dependence of the Quark Distributions in QCD. *Nucl. Phys. B* **1979**, *151*, 421–428. [CrossRef]
161. Gribov, V.N.; Lipatov, L.N. Deep inelastic e p scattering in perturbation theory. *Sov. J. Nucl. Phys.* **1972**, *15*, 438–450.
162. Gribov, V.N.; Lipatov, L.N. e+e-pair annihilation and deep inelastic e p scattering in perturbation theory. *Sov. J. Nucl. Phys.* **1972**, *15*, 675–684.
163. Lipatov, L.N. The parton model and perturbation theory. *Sov. J. Nucl. Phys.* **1975**, *20*, 94–102.

164. Altarelli, G.; Parisi, G. Asymptotic Freedom in Parton Language. *Nucl. Phys. B* **1977**, *126*, 298–318. [CrossRef]

165. Dokshitzer, Y.L. Calculation of the Structure Functions for Deep Inelastic Scattering and e+ e- Annihilation by Perturbation Theory in Quantum Chromodynamics. *Sov. Phys. JETP* **1977**, *46*, 641–653.

166. Krivokhizhin, V.G.; Kotikov, A.V. Functions of the nucleon structure and determination of the strong coupling constant. *Phys. Part. Nucl.* **2009**, *40*, 1059–1099. [CrossRef]

167. Illarionov, A.Y.; Kotikov, A.V.; Bermudez, G.P. Small x behavior of parton distributions. A Study of higher twist effects. *Phys. Part. Nucl.* **2008**, *39*, 307–347. [CrossRef]

168. Kotikov, A.V. Deep inelastic scattering: Q**2 dependence of structure functions. *Phys. Part. Nucl.* **2007**, *38*, 1–40; Erratum in *Phys. Part. Nucl.* **2007**, *38*, 828. [CrossRef]

169. Chetyrkin, K.G.; Tkachov, F.V.; Gorishnii, S.G. Operator Product Expansion In The Minimal Subtraction Scheme. *Phys. Lett. B* **1982**, *119*, 407–411. [CrossRef]